

Bowdoin College

## Bowdoin Digital Commons

---

Honors Projects

Student Scholarship and Creative Work

---

2023

### Diatom blooms in Harpswell Sound: seasonality, succession, and origin

Charlie Francis O'Brien  
*Bowdoin College*

Follow this and additional works at: <https://digitalcommons.bowdoin.edu/honorsprojects>



Part of the [Biogeochemistry Commons](#), [Environmental Monitoring Commons](#), and the [Marine Biology Commons](#)

---

#### Recommended Citation

O'Brien, Charlie Francis, "Diatom blooms in Harpswell Sound: seasonality, succession, and origin" (2023). *Honors Projects*. 467.  
<https://digitalcommons.bowdoin.edu/honorsprojects/467>

This Open Access Thesis is brought to you for free and open access by the Student Scholarship and Creative Work at Bowdoin Digital Commons. It has been accepted for inclusion in Honors Projects by an authorized administrator of Bowdoin Digital Commons. For more information, please contact [mdoyle@bowdoin.edu](mailto:mdoyle@bowdoin.edu), [a.sauer@bowdoin.edu](mailto:a.sauer@bowdoin.edu).

Diatom blooms in Harpswell Sound: seasonality, succession, and origin

An Honors Paper for the Department of Earth and Oceanographic Science  
by Charlie Francis O'Brien

Bowdoin College, 2023  
© 2023 Charlie Francis O'Brien

## Table of Contents

<i>Acknowledgments</i> .....	<i>iii</i>
<i>Preface</i> .....	<i>iv</i>
<i>Abstract</i> .....	<i>v</i>
<i>List of Abbreviations</i> .....	<i>vi</i>
<b>1 Introduction</b> .....	<b>1</b>
<b>2 Background</b> .....	<b>3</b>
2.1 Diatom phylogeny, evolution, and life history .....	3
2.2 The Gulf of Maine and Harpswell Sound .....	7
2.3 Toxic blooms .....	9
<b>3 Research Questions and Hypotheses</b> .....	<b>12</b>
3.1 Seasonal blooms in Harpswell Sound .....	12
3.2 Successional patterns in Harpswell Sound.....	16
3.3 Origin of diatom blooms in Harpswell Sound .....	19
3.4 Changing composition of toxic blooms in Harpswell Sound .....	22
<b>4 Methods</b> .....	<b>23</b>
4.1 Sites, Platforms, and Time Intervals .....	23
4.2 Data and Instrumentation .....	24
4.3 Data Analysis .....	26
<b>5 Results</b> .....	<b>30</b>
5.1 Seasonal blooms .....	30
5.2 Successional patterns .....	36
5.3 Origin of diatom blooms .....	37
5.4 Changing composition of toxic blooms.....	42
<b>6 Discussion</b> .....	<b>45</b>
6.1 Seasonal blooms.....	45
6.2 Succession patterns.....	48
6.3 Origin of diatom blooms .....	50
6.4 Changing composition of toxic blooms.....	51
6.5 Future directions .....	53
<b>7 Summary</b> .....	<b>55</b>
<i>Supplementary material</i> .....	<i>56</i>
<i>References</i> .....	<i>60</i>

## **Acknowledgments**

I am very grateful for Collin Roesler, who advised this project at all stages and made it a valuable learning process. Thank you, Sue Drapeau, for great company and technical help with plankton imaging. Thank you to Heidi Franklin and the staff at the SCSC for maintaining the flowing seawater lab by pigging, among many other ways. Thank you to Michael Brosnahan at WHOI for the HABON-NE dataset and for answering questions about it. Thank you to committee members Emily Peterman and Phil Camill for offering thoughtful comments on a draft. This work was funded by the Surdna Foundation Undergraduate Research Fellowship and the Grua/O'Connell Research Award. I acknowledge support from NASA Ocean Biology and Biogeochemistry and NOAA for acquisition and support of operations of the IFCB, respectively.

## **Preface**

What is now called Harpswell by most was the territory of the Pejepscot, a subtribe of the Arosagunticooks, themselves a part of the Abenaki tribe, who, after European colonization, joined other Maine tribes to form the Wabanaki (Dawnland Confederacy). The Abenaki tribe is not officially recognized in the United States because many Abenakis fled to Quebec in the 17th and 18th centuries prompted by colonial violence. Before beginning this paper, I acknowledge that Harpswell is the traditional land of the Abenaki.

The Wabanaki's right to self-governance and sovereignty in these lands is federally recognized but has not been recognized by the State of Maine since 1980. For 43 years, federal legislation passed for the benefit of indigenous tribes has excluded the Maine tribes. We should all support legislation that gets the state to recognize the existence of the Abenaki, recognize indigenous tribal sovereignty, and allow federal benefits to apply to people indigenous to Maine.

## Abstract

Harpwell Sound (HS) is an inlet in northeastern Casco Bay that exerts control on Gulf of Maine ecosystem health, yet its complex phytoplankton community dynamics have not been characterized with sufficiently detailed analyses. In this research, high-resolution automated microscopy and current velocity observations were used to test the seasonality, ecological succession, bloom origin location, and potential toxicity of populations in HS between 2020 and 2022. Winter months could exhibit slow accumulation of diatom biovolume. Cold, salty surface water has net outflow in winter as nutrients from depth are replenished during net upwelling conditions, and populations could be exported from the inlet at the surface. Extreme current velocity variability in spring due to the Kennebec River plume in HS destabilizes spatially uniform populations. Warm, low-salinity surface water with net inflow in summer (net downwelling which retains populations at the head of the sound) corresponds with temporally separate dinoflagellate and diatom blooms. Large, multi-peaked spring and fall diatom blooms are recurrent, contrasting small, short-lived blooms in summer. A successional pattern from diatoms to dinoflagellates is confirmed for summer but refuted for other seasons. The hypothesis that diatom succession during all blooms in HS is characterized by large centric cells preceding small cells or pennate cells was explored but no clear pattern in decreasing cell size was observed. Observed tidal effects on biovolume concentration could mask that blooms develop at coherent times but spatially separated. A diverse community of toxic phytoplankton, including dinoflagellates and *Pseudonitzschia*, are observed throughout the year.

## **List of Abbreviations**

HS: Harpswell Sound

IFCB: Imaging FlowCytoBot

SCSC: Schiller Coastal Studies Center (Orrs Island, Maine)

LOBO: Land Ocean Biogeochemical Observatory (Harpswell Sound, ME)

HAB: Harmful algal bloom

GOM: Gulf of Maine

## 1 Introduction

In continental shelf seas, photosynthesizers use approximately 8 TW of solar energy—the equivalent of half of humanity’s global energy demand (Simpson & Sharples 2012)—to make their own food. Some of this energy, in the form of biomolecules, moves through the food web to zooplankton, fish, and shellfish, supporting a wide-ranging and economically robust marine ecosystem. When particulate organic carbon originating from phytoplankton production at the sea surface sinks to the seafloor, it drives the biological carbon pump, the process of carbon transport from the atmosphere to the geosphere via the biosphere (Martin et al. 2011). Carbon stored over deep time in this way exerts a control on atmospheric CO<sub>2</sub> concentration and contributes to petroleum reserves (Shukla & Mohan 2012; Tulan et al. 2020; Jang et al. 2022). The diatoms (*Bacillariophyta*) contribute significantly to productive ecosystems and carbon sequestration (Benoiston et al. 2017); they produce more atmospheric oxygen than all the Earth's rainforests (Hennon et al. 2015) and are the dominant export taxon (Irion et al. 2021).

An investigation into the dynamics of diatom taxa concentration fluctuations is required to better understand how they contribute to local fisheries and the global carbon balance. Harpswell Sound (HS) is a place to test how coastal phytoplankton communities compare or contrast with communities in the Gulf of Maine (GOM) and North Atlantic Ocean more broadly. Is this coastal ecosystem of HS unique in its diatom abundance dynamics, or are the processes known to govern diatom abundance more broadly conserved in this inlet?

An analysis of the temporal variability of diatom taxa concentration on the scale of hours to years in Harpswell Sound, Maine, guides this investigation in which the following specific questions are addressed:

(1) Does HS have predictable seasonal blooms of diatoms? If so, are they coherent with and well-described by the chlorophyll concentration peaks observed during spring and fall in the broader Gulf of Maine (Song et al. 2010) and North Atlantic (Martinez et al. 2011), and do they have the same drivers predicted by the Sverdrup (1953) critical depth hypothesis and the Evans & Parslow (1985) annual mode of plankton cycles?

(2) Can phytoplankton taxa succession within HS be characterized by the Margalef mandala (1978), which describes the sequence of diatoms followed by dinoflagellates? Is there a consistent pattern of diatom taxa succession across distinct blooms from large cells (e.g., *Thalassiosira*) to smaller cells (e.g., *Chaetoceros*), as more recent studies have confirmed (Kemp & Villareal, 2018; Suzuki et al. 2021)?

(3) Does the onshore or offshore environment offer more suitable conditions for the development of diatom blooms? Or does taxa biovolume uniformly grow across estuarine space during blooms in accordance with a well-mixed physical structure? In other words, are inlets subject to the same drivers as offshore water or are they unique ecosystems with responses to local controls?

(4) Is the most abundant toxic phytoplankton in HS *Alexandrium*, given that shellfish become toxic due to this taxa on a near-yearly basis and this taxa is thought to be indigenous to HS (Bean et al. 2005)? Do low-nutrient summer conditions facilitate toxic blooms in HS? Or do blooms occur earlier given that HS has previously been the first area in Maine that shows toxicity (Bean et al. 2005)?

## **2 Background**

### *2.1 Diatom phylogeny, evolution, and life history*

An endosymbiotic event between a eukaryotic cell and a photosynthetic cyanobacteria took place 1.5 billion years ago, resulting in the ancestor of terrestrial plants and red and green algae. A second endosymbiotic event occurred around 1 billion years ago in which a eukaryotic heterotroph engulfed a red alga and possibly also a green alga, creating the common ancestor for single-celled phytoplankton, seaweeds, and plant parasites. Diatoms are a taxonomic class of phytoplankton in the kingdom Protista (Figure 1). Although photosynthetic, they are not plants. Although eukaryotic, they are not animals nor fungi. Diatoms have evolved and continue to evolve by gaining and losing bacterial genes (Amin et al. 2012) and fragments of viral genes (Hongo et al. 2021).

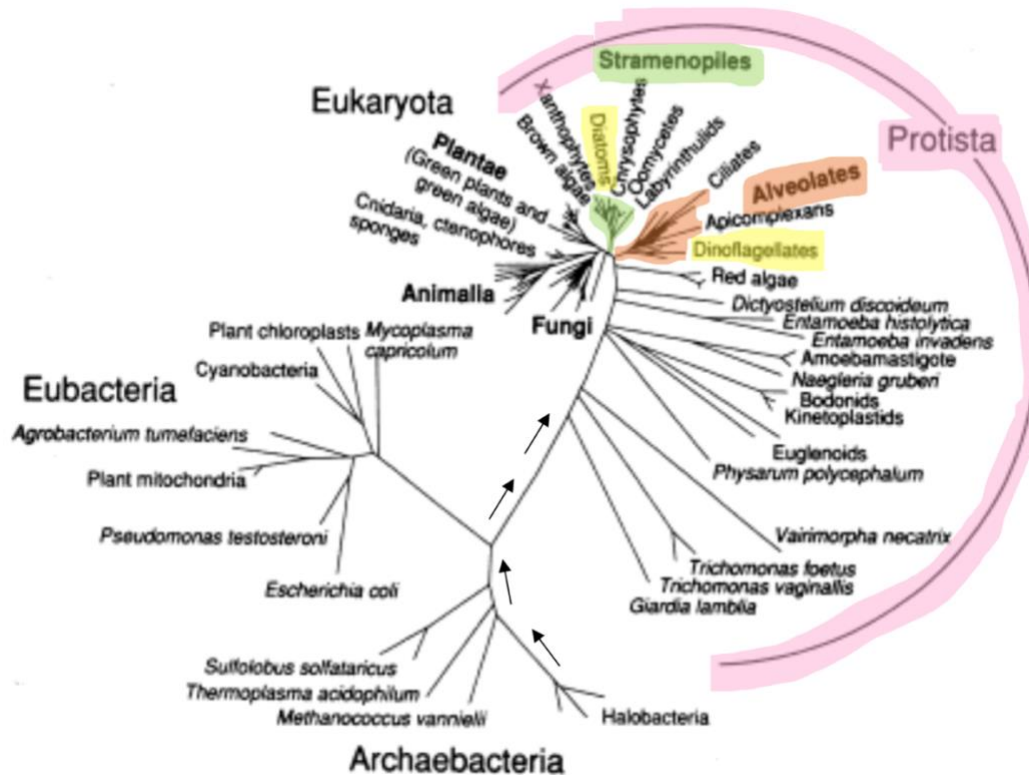


Figure 1. A phylogenetic tree of biological taxonomic groups on Earth. Most biological diversity on Earth is accounted for in the kingdom Protista (highlighted in pink). The Alveolate and Stramenopile groups (green), which include all the phytoplankton taxa, including diatoms and dinoflagellates (yellow), are eukaryotes that evolved separate from plants, fungi, and animals. Figure adapted from Dawson (2011).

The diatoms generally fall into the largest size class of phytoplankton, the microplankton (>20  $\mu\text{m}$  in length), with some species in the nanoplankton size class (2-20  $\mu\text{m}$ ). They are characterized by two-part silica cell walls called frustules that act to protect them from predators (Yoshida et al. 2004; the Greek word *diatomos* means "cut in half"). Cells are classified into two general morphologies: centric or pennate (Figure 2a). Cells exist in both solitary and colonial forms, with chains of cells growing up to mm-scale lengths (Figure 2b).

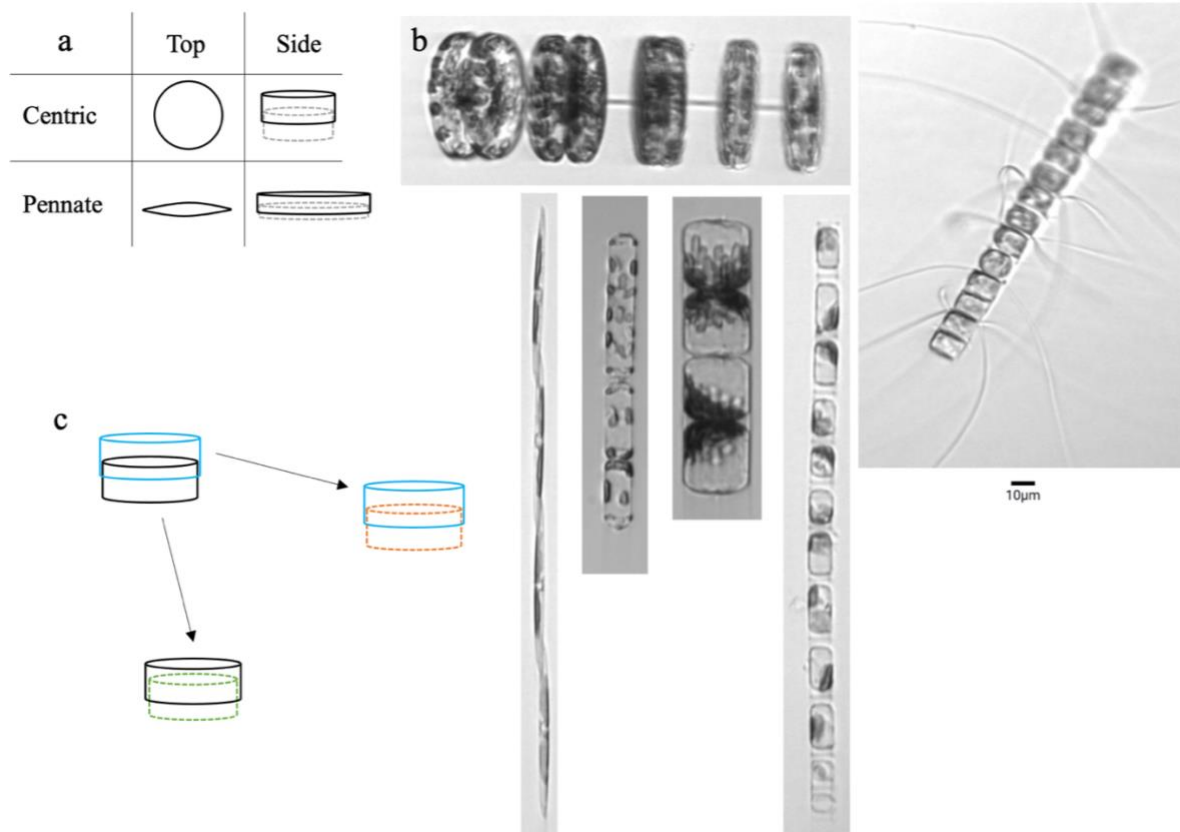


Figure 2. The two morphologies of diatoms (a). Example images of diatom taxa from Harpswell Sound in 2020-2022 (b). Clockwise from top left: *Thalassiosira*, *Chaetoceros*, *Skeletonema*, *Guinardia delicatula*, *Cerataulina pelagica* and *Pseudonitzschia*. Mitotic division is especially evident in *Thalassiosira* and *Guinardia delicatula* pictured here. All taxa have formed chains of multiple cells. Asexual reproduction of a centric diatom involves the separation of frustules and the synthesis of new inner cell walls for each frustule, forming two daughter cells (c).

There are probably 200,000 extant species of diatoms (Armbrust 2009) that have evolved to occupy specific ecological niches throughout the world's oceans (Malviya et al. 2016).

Diatoms thrive in well-mixed waters of high-latitude and polar regions, where high nutrient levels support their larger cell size compared to other phytoplankton. Diatoms are estimated to have arisen 250 Ma (Armbrust 2009). Fossils are preserved from 190 Ma but species diversification did not start to increase dramatically until the Cretaceous (~100 Ma), when the supercontinent Pangea was separating to form the modern ocean basins (Benoiston et al. 2017; Westacott et al. 2021). Centric diatoms first contributed significantly to carbon cycling at this

time by inhabiting the well-lit floor of shallow seas. They then evolved to inhabit offshore surface waters that provided nutrients from the weathering continents. Centrics survived the Cretaceous mass extinction (66 million years ago) and evolved to be able to inhabit reduced nutrient conditions in the open ocean, leading to the evolution of the pennate group about 30 Ma (Armbrust 2009).

The circumpolar sea opened around Antarctica 34 million years ago and sent Earth into an ice-house period, causing diatoms to benefit from an altered ocean thermal structure. Diatoms flourish in colder water because it is often well-mixed with nutrients. They have evolved a nutrient storage vacuole which allows continued cell division under nutrient limiting conditions. From an earth systems perspective, diatoms outcompete all other phytoplankton in glacial periods (like the present) in which temperature gradients are greatest between the equator and poles. Sufficient frequency of high winds and storms that mix nutrients to the surface in pulses allow diatoms to absorb and store the nutrients they will need during ensuing low-nutrient conditions (Falkowski & Oliver 2007).

Diatom populations propagate by asexual and sexual modes of reproduction. Asexual reproduction, which occurs during blooms, is the binary fission of independent cells (also called cloning). Cell division divides the cell wall into the two halves, yielding two daughter cells. Each synthesizes a new inner cell wall. Subsequent divisions lead to a population with sequentially decreasing size of the daughter cell (Figure 2c). Cell division continues to take place as long as the cell is large enough to split, after which sexual reproduction takes place. Maximum cell size is achieved again by sexual reproduction, in which the combination of gametes form an auxospore. Mouget et al. (2009) found that sexualization of the marine diatom *Haslea ostrearia* occurs most likely in low light and low photoperiod conditions of winter and suggest that

brighter conditions during spring and fall are correlated with cloning. In 2013, *Pseudonitzschia multistrata* in the Gulf of Naples, Italy, diversified its gene pool through high rates of sexual reproduction over cloning. However, cloning was the predominant mode of reproduction in blooms. Clonal population expansion during blooms causes distinct differences in genetic compositions across bloom populations (Ruggiero et al. 2022).

## *2.2 The Gulf of Maine and Harpswell Sound*

Harpswell Sound extends out of Brunswick, Maine, between a long peninsula and a series of islands within northeastern Casco Bay and the broader Gulf of Maine (GOM; Figure 3a). The Western Maine Coastal Current (WMCC) direction and magnitude vary with the degree of connectivity with the Eastern Maine Coastal Current, which promotes southwestward flow past HS (Figure 3b). Mean flow southwestward opposes the mean wind stress northeastward throughout the spring and summer seasons (Pettigrew et al 2005). In contrast, strong winds out of the southwest in late fall and in winter counteract the current and pile up water in Wilkinson Basin, creating coastal northeastward flows (Li et al. 2022).

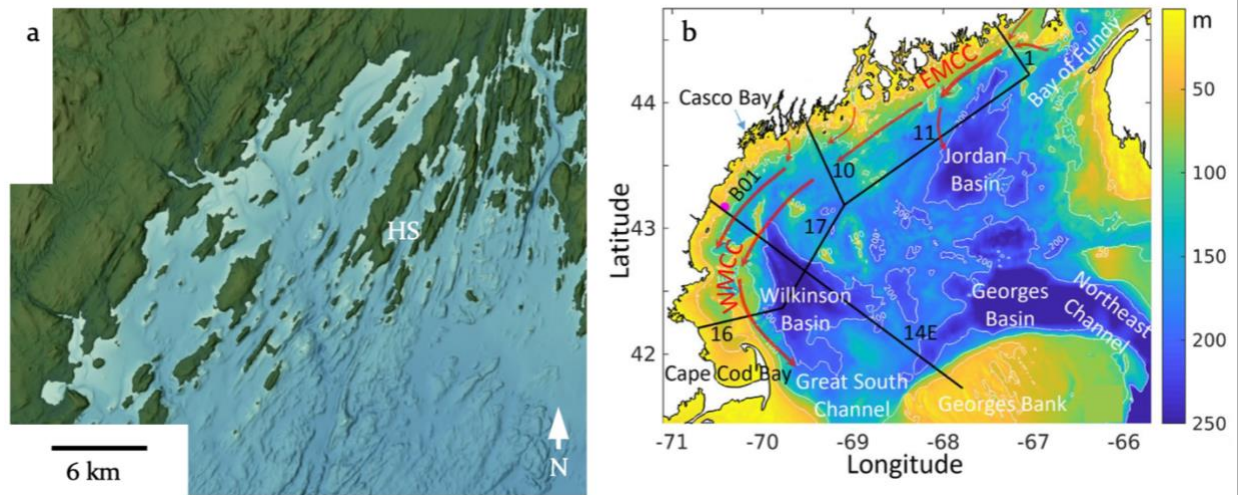


Figure 3. Casco Bay bathymetry, with HS located in the northeast (a). Gulf of Maine bathymetry with 200 m, 100 m, and 50 m isobaths (white lines) and coastal currents (b). The Eastern Maine Coastal Current (EMCC) and the Western Maine Coastal Current (WMCC) flow southwest along the coast (large red arrows) and are fed by Penobscot River and Kennebec River outputs (small red arrows), the latter of which is adjacent to northeast Casco Bay. (a) is adapted from the National Centers for Environmental Information (NCEI) DEM Global Mosaic and (b) is adapted from Li et al. 2022 Figure 1 (numbers refer to transects in their study).

Peabody (2014) quantified Gulf of Maine circulation patterns along the coast over a typical year. Baseline surface flow of 2 to 6 cm/s toward the southwest was observed at buoys 50 km east and 35 km south of the mouth of HS. Southwest surface water flow accelerated in the spring and summer and the fastest flows were always at the surface at these two locations. At the buoy 35 km south of the mouth of HS, peak flow southwest occurred March 31st through May 31st (7cm/s); slight flow toward the northeast was observed September 7th to December 6th; the cross-shore flow was toward offshore throughout the year. At the buoy 50 km north of the mouth of HS, peak flow southwest was observed May 5th through July 19th (11cm/s), and along-shore flow was always southwestward. Cross-shore flow toward onshore occurred March 16th through September 7th and was toward offshore the rest of the year (Figure S1).

There is no observed freshwater source at the head of HS but rather a strong freshwater source at the mouth of HS from an advected river plume. A source of freshwater to the GOM are Maine rivers, such as the Kennebec River and Penobscot, most notably (Wolovick et al. 2008;

Pettigrew et al. 2005). The propagation of river plumes of lower salinity water into the Gulf of Maine is dependent on river inflows, wind stresses (Fong et al. 1997), and GOM currents. Sometimes the Kennebec River plume is imported into HS by the WMCC and appears as turbid, freshened water (Carberry et al. 2019). The plume provides silicate to the sound, but minimal phosphate and forms of nitrogen, which are limiting nutrients. Therefore, it is not rivers but deep shelf sea mixing that contributes most nutrients to the Harpswell Sound phytoplankton community (Ballance 2020).

An investigation into the decline in chlorophyll concentration in most of the world's oceans since 1900 has determined that increases in sea surface temperature are generally related to phytoplankton decline due to increased stratification and isolation of deep nutrient sources. While most of the open ocean has warmed by less than 1 °C since 1900, the Gulf of Maine has warmed by 1.5 °C (Boyce et al. 2010), which is the fastest recorded warming in its last 1000 years (Whitney et al. 2022). Since the 1970s, the GOM has received colder and fresher water from the Labrador Current and less Warm Slope Water through the Northeast Channel as the melting of the Arctic strengthens the Labrador Current (Townsend et al. 2010). The Labrador current has a concentration of silicate that facilitates diatom growth better than Warm Slope Water, and its temperature is also more optimal for the growth of subpolar taxa.

### 2.3 Toxic blooms

Some phytoplankton taxa can produce toxins under nutrient limiting conditions (Frangópulos et al. 2004) or as an anti-grazing function (Selander et al. 2006). The only known toxic diatoms fall into the genus *Pseudonitzschia* and produce the neurotoxin domoic acid, which has caused deadly Amnesic Shellfish Poisoning in humans and other animals that ingest poisoned shellfish (Ansdell 2019). Thirty percent of the taxa within the genus *Pseudonitzschia*

are known to produce domoic acid and may contribute to harmful algal blooms (HABs), during which shellfish harvesting operations should be closed to prohibit human poisoning and access to the coast should be limited (Bean et al. 2005).

Dinoflagellates are a group of phytoplankton (Figure 1) that reached peak species diversity in the Mesozoic (250 to 66 million years ago; Delwiche 2007). The Mesozoic was a hothouse period for Earth, facilitating stratified oceans that dinoflagellates could exploit. (The Cenozoic decline in global temperature has increased ocean mixing to the detriment of dinoflagellates.) Extant dinoflagellates are single-celled phytoplankton that can vertically migrate using their flagella toward light or nutrients, if needed (Wirtz et al. 2022). They grow slowly and are competitive in nutrient-depleted water typical of stratified zones, specifically if diatoms are silicate limited (Flynn et al. 2012; Dolan 1992).

Known toxic dinoflagellates that produce HABs include *Alexandrium*, which causes Paralytic Shellfish Poisoning (PSP; DMR 2022) by producing Saxitoxins (Valbi et al. 2019), and *Dinophysis*, which causes Diarrhetic Shellfish Poisoning (DSP; DMR 2022) by producing okadaic acid and dinophysistoxins (WHOI 2019). Decades of research has focused on HAB species in the Gulf of Maine, but most of that research has investigated *Alexandrium* (a google scholar search for "*Alexandrium* Gulf of Maine" yields ~3,600 results) and less has investigated *Pseudonitzschia* (~1,700 results) and *Dinophysis* (~1,700 results).

Historically in Maine, HABs have occurred between April and October (DMR 2022). HABs are predicted to increase in frequency in the coastal ocean because of warming, loss of predators, and sustained nutrient supply from terrestrial run off (Armbrust 2009). A historic, gulf-wide bloom of the toxic diatom *Pseudonitzschia australis* occurred in 2016 (Clark et al. 2021). HABs of *Alexandrium fundyense* (now *catenella*) that originate in Lombos Hole, an

embayment within HS, are recorded by a biotoxin monitoring station of the Department of Marine Resources (Bean et al. 2005). However, identifying origins of phytoplankton blooms is not the monitoring system's goal, so the use of data presented in this study can also be used to better understand toxic phytoplankton dynamics in this region.

### **3 Research Questions and Hypotheses**

#### *3.1 Seasonal blooms in Harpswell Sound*

The seasonal cycle of phytoplankton abundance has been documented for over a century in the Gulf of Maine and the Atlantic Ocean in the approximate latitude of Harpswell Sound using a range of approaches, from net microscopy and analysis of chlorophyll to optical measures of chlorophyll fluorescence. Satellite imagery has more recently been the most feasible method to quantify chlorophyll across the oceans because discrete sampling of locations is time consuming, costly, and low resolution. Because chlorophyll concentration is a proxy for phytoplankton biomass that can be detected from satellite-based sensors, Song et al. (2010) analyzed satellite ocean color data of the Gulf of Maine from 1998 to 2008 using numerical modeling to determine when chlorophyll concentration peaks occurred. In Wilkinson Basin, which is 150 km SSE of the mouth of Harpswell Sound (Figure 3), chlorophyll concentrations peaked on April 10 and October 7, on average. Corroborating evidence for a fall peak consistently lower than a spring peak comes from a study that quantified distinct phytoplankton groups within a community by genetic sequencing and imaging flow cytometry analysis (Bolaños et al. 2020), which found that diatom biomass in North Atlantic subtropical and subpolar locations is up to six-fold greater in spring than it is in winter. Coastal waters are more productive than the Gulf of Maine and North Atlantic during seasonal blooms (Song et al. 2010), but it is uncertain if the coastal zone follows a seasonal pattern of blooming, a random pattern, or if it maintains a consistent level of production throughout the year.

Predictable changes in stratification and mixing offshore are physical mechanisms that facilitate spring and fall phytoplankton blooms in the Gulf of Maine. In winter, low air temperatures cause surface water density to become colder and equilibrate with deeper water,

which creates uniform density. More frequent storms in winter easily overturn water in this density regime, bringing nutrient-rich deep water to the surface and diluting surface phytoplankton populations. In spring, sunlight warms surface water and decreases its density, creating stratification between the surface and higher density deep water (Evans & Parslow 1985). As summer begins, Sosik et al. (2001) observed subsurface maxima of chlorophyll and particulate matter, indicating that a surface layer with distinct physical properties had developed. As phytoplankton grow, they deplete the nutrients down to low concentrations in an immobile surface layer, which creates a subsurface maximum of phytoplankton concentrated at the base of the surface layer adjacent to the higher nutrient waters underlying the surface layer. It is the delicate balance of phytoplankton being held up to sufficient light by stratification when there are enough nutrients around that informs the spring and fall bloom hypothesis. Concentration of nutrients and degree of stratification behave inversely across seasons in the Gulf of Maine. Peaks in chlorophyll concentration in Wilkinson Basin during spring and fall indicate that there are sufficient nutrient concentrations and sufficient stratification to maintain high production in the photic zone (Figure 4).

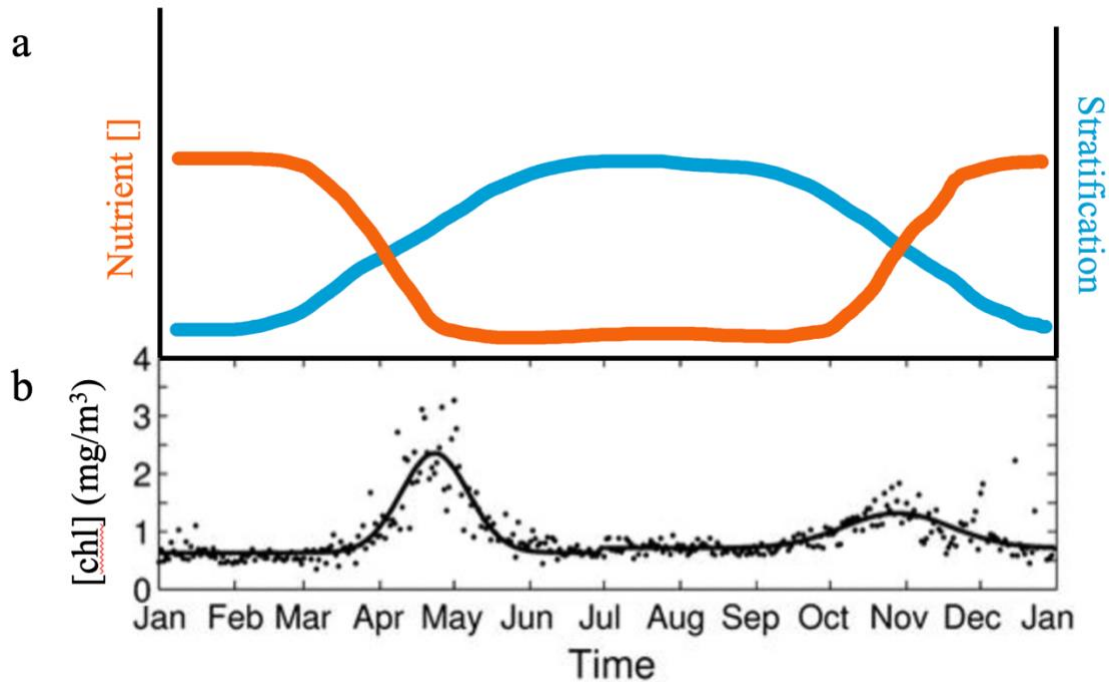


Figure 4. The concentration of nutrients in surface water and the degree of stratification in Wilkinson Basin over a typical year (a). Satellite-based estimates of daily average chlorophyll concentration in Wilkinson Basin from 1998 to 2008 (b). (a) is informed by Evans & Parslow (1985) and (b) is adapted from Figure 3 of Song et al. (2010).

In contrast to predictable offshore Gulf of Maine water column physics throughout the year, coastal phytoplankton production lends itself to physical conditions of sea water changing over relatively short distances. Solar heating and freshwater input (from rain and/or rivers) stratify the water column into layers with distinct densities by inducing thermal expansion of surface water or by introducing low density freshened surface water, respectively. Breaking down the stratification requires energy from tides or wind. Distinct layers within the water column may have different velocities, creating shear, which in turn causes the propagation of turbulence, stirring the seawater to a more uniform density (Falkowski & Oliver 2007). Both winds and tidal currents can induce velocity shear. Notable changes in tidal stirring due to shoaling bathymetry cause a tidal mixing front to form at the bathymetric slope (Simpson & Sharples 2012). Tides can mix the entire water column in shallow water, redistributing nutrients

formerly concentrated at the seafloor towards the surface, allowing phytoplankton to flourish because of the simultaneous access to sufficient nutrients and light. Offshore of the slope, tidal energy is dissipated over depth and stratification occurs (Figure 5). Significant wind events, however, can move the tidal mixing front offshore because of the energy that they add to the surface can mix the sea surface down to tidally mixed depths.

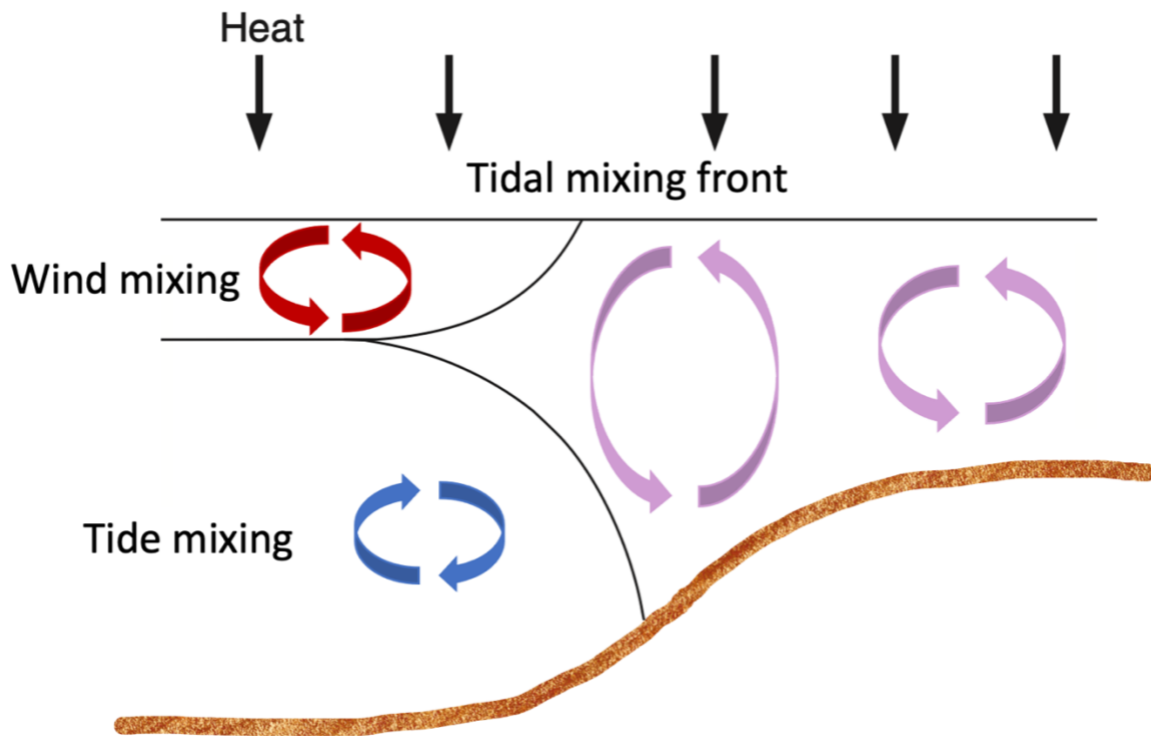


Figure 5. A sketch of the bathymetric slope and consequent tidal mixing front in a coastal ocean. Adapted from Simpson & Sharples 2012.

Although one might predict a continuous level of coastal production, investigations into the seasonal patterns of coastal phytoplankton abundance have yielded mixed results. Using imaging flow cytometry, Hunter-Cevera et al. (2019) found that the abundance of *Synechococcus*, a marine picocyanobacterium, at Martha's Vineyard Coastal Observatory in

Massachusetts was strongly seasonal from 2003 through 2018. The species consistently bloomed in spring (April-May-June) and underwent summer cycling in abundance and total biovolume before fading in the fall (without a bloom) and waning further in the winter. Nevertheless, using satellite-derived chlorophyll concentration, Marchese et al. (2022) determined that spring bloom timing varies in the open and coastal oceans of British Columbia and Southeast Alaska across bioregions and interannually. The spring bloom in inner coastal waters took place between late March and early April. Inferred influences of zooplankton grazing, upwelling, tidal mixing, and freshwater input make the appearance of coastal ocean spring and fall blooms less pronounced. This study provides some insight into the possible variability of Harpswell Sound diatom seasonality, which has yet to be studied.

The first hypothesis (H1): *Harpswell Sound, having comparable seasonal nutrient and light regimes as the subpolar North Atlantic and greater Gulf of Maine, will exhibit a single spring bloom and fall bloom, with the magnitude of the spring bloom exceeding that of the fall bloom.*

### *3.2 Successional patterns in Harpswell Sound*

Phytoplankton groups have evolved capabilities to differently exploit specific water column physical and chemical conditions. It is yet to be determined whether the changing conditions of HS align with predicted changes in HS phytoplankton groups from a canonical open-ocean ecosystem model. Given that phytoplankton succession is comparable to the terrestrial ecological succession of grasslands to forests (Madin 2005), understanding the complexity of phytoplankton succession pathways under distinct environmental conditions is important from the perspective of the differing roles these taxa play in structuring the ecosystem to their biogeochemical use.

Phytoplankton succession has been described historically by an ecological model established by Margalef (1978), called the Margalef mandala (Figure 6). The model describes the seasonal succession of major phytoplankton classes and of genera within classes in response to evolving physical and chemical conditions; specifically, the succession from diatom to dinoflagellate taxa as stratification occurs and nutrients are depleted. Diatoms tend to thrive in turbulent and nutrient-rich waters, often forming fast-growing chains of cells that rely on mixing to interact with nutrients and to get to the surface to receive light. Diatoms were thought of as non-motile taxa that were not selected for in stratified waters, as "non-motile cells sink fatally in low turbulence waters and the population disappears. In such an environment, it pays for the organism to invest some energy in swimming around, and it helps if the species are well defended against animals" (Margalef, 1978).

Reexaminations of the model recognize the importance of variables other than nutrient concentration and turbulence on succession, such as cell size, nitrogen form preference, growth rate (Gilbert 2016), and selective grazing of taxa by zooplankton, which is known to occur in the Northeast Atlantic Ocean (Gaul & Antia 2001; Zheng et al. 2022). Nutrient uptake efficiency increases with smaller cells because of increased cell surface-area-to-volume ratio, so while nutrients decline smaller taxa are predicted to follow bigger taxa in succession. Such a pattern was observed in the summer of 2013 in the northern Bering Sea, in which *Chaetoceros* cells three to six times smaller than *Thalassiosira* cells numerically dominated stratified waters over *Thalassiosira*, whose biomass increased only when stratification decreased (Suzuki et al. 2021). In another case, Sosik et al. (2001) observed smaller and smaller cells inhabiting the surface layer of a stratified water column on the New England continental shelf in the summer of 1996.

A proposed diatom succession sequence based on previous observations that highlight the importance of cell size is indicated by the blue box in Figure 6.

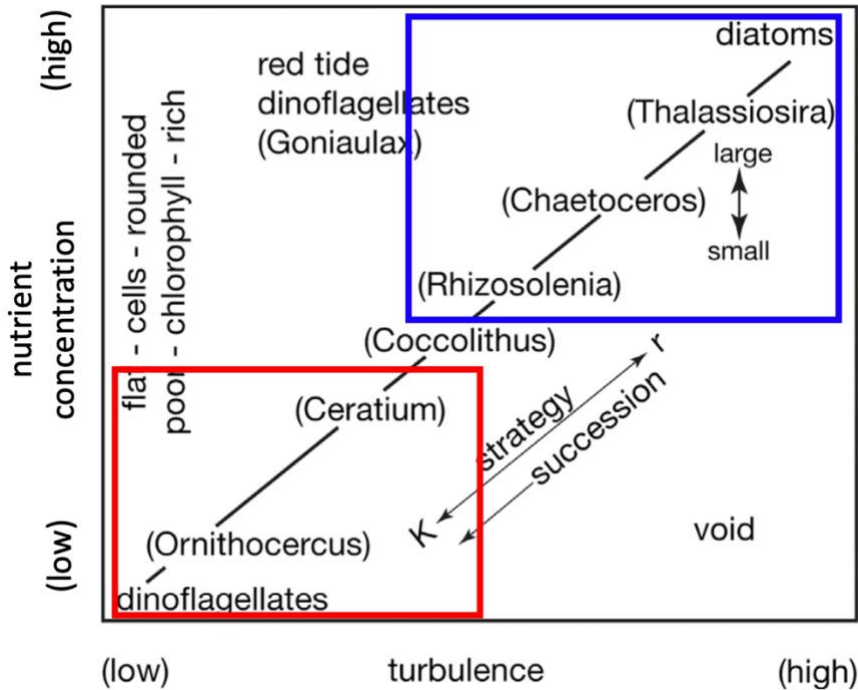


Figure 6. The phytoplankton groups that have evolved to flourish in distinct nutrient concentration and turbulence regimes. Arrows describe ecological succession and ecosystem strategies. The description on the vertical axis describes cell characteristics that correspond to ambient nutrient concentration. Diatom taxa shown are within the blue box and dinoflagellate taxa are within the red box. Adapted from Figure 1 of Kemp & Villareal (2018), after Figure 2 in Margalef (1978).

However, Kemp & Villareal (2018) conclude that some diatom taxa account for nutrient-depleted conditions with different growth strategies, which potentially adds more complexity to the model of succession based on cell size. Buoyancy regulation through ion exchange (Gemmel et al., 2016; Kemp et al., 2000) can increase nutrient concentration gradients at cell boundaries when cells are nutrient depleted (a necessity that formerly relied on abiotic turbulence transporting nutrients to the surface of the cell; Falkowski & Oliver 2007). Buoyancy regulation can also be used to mine nutrients up to 100 m deep in the open ocean (Armbrust 2009). Other

growth strategies are photosynthetic adaptation to lower light levels at depth and symbiosis with N-fixing cyanobacteria.

Phytoplankton succession is even more complex to study because of the unknown dynamics of taxa migration across locations (Gleason 1926). Coastal zones at similar latitudes and with similar physical regimes can vary distinctly in diatom taxa abundance and succession throughout the year (Luostarinen et al. 2020). Perhaps even slightly different initial taxonomic compositions of diatom communities are amplified over time. Harpswell Sound diatom taxa succession patterns are worth investigating more deeply to better understand the local drivers of ecological change, but what is learned from this coastal zone may be applicable to similar coastal geographies in Maine and even further to other subpolar coastal environments.

The second hypothesis addresses succession. H2a: *Harpswell Sound diatom taxa biovolume will follow a consistent successional pattern to dinoflagellates: when the bloom declines, dinoflagellate biovolume will increase in response.* H2b: *During all diatom blooms succession takes place from large centric cells (e.g., Thalassiosira) to small cells (e.g., Chaetoceros) or pennate cells (e.g., Pseudonitzschia).*

### *3.3 Origin of diatom blooms in Harpswell Sound*

There are three distinct scenarios for diatom bloom origin: uniform distribution from onshore to offshore locales consistent with the theory that inlets are mere extensions of offshore waters, offshore source and onshore transport consistent with the idea that inlets do not provide conditions to initiate or retain populations, or onshore source with offshore transport consistent with the theory that inlets are incubators for phytoplankton development (Bean et al. 2005). Distinguishing between these scenarios depends upon the observational platforms. In the absence of remote sensing that is highly resolved both temporally and spatially, which is not currently

available, moored sensors provide the best approach. For the scenario in which a population is uniformly distributed within and outside the sound, the movement of water with tides would not affect the concentration of the population recorded at a location within HS (Figure 7 a, b), and so the concentration would hypothetically remain constant between high and low tides.

The other two scenarios entertain the possibility of detection of a bloom that has originated offshore of the sampling location or upstream of the sampling location. If an offshore bloom infiltrates into the sound, the population might appear more concentrated at the sampling location during high tide because there is a chance that the bloom has traveled inland with the flowing tide. Conversely, if there is a bloom upstream of the sampling location, we might expect the concentration of the population to appear greater during low tide, when the ebbing tide has possibly advected that concentrated bloom downstream to the sampling location. These predictions draw on the findings of previous investigators (Cross et al. 2015; Kimmerer et al. 2014; Yelton et al. 2022) that demonstrate the transport of plankton by tidal currents.

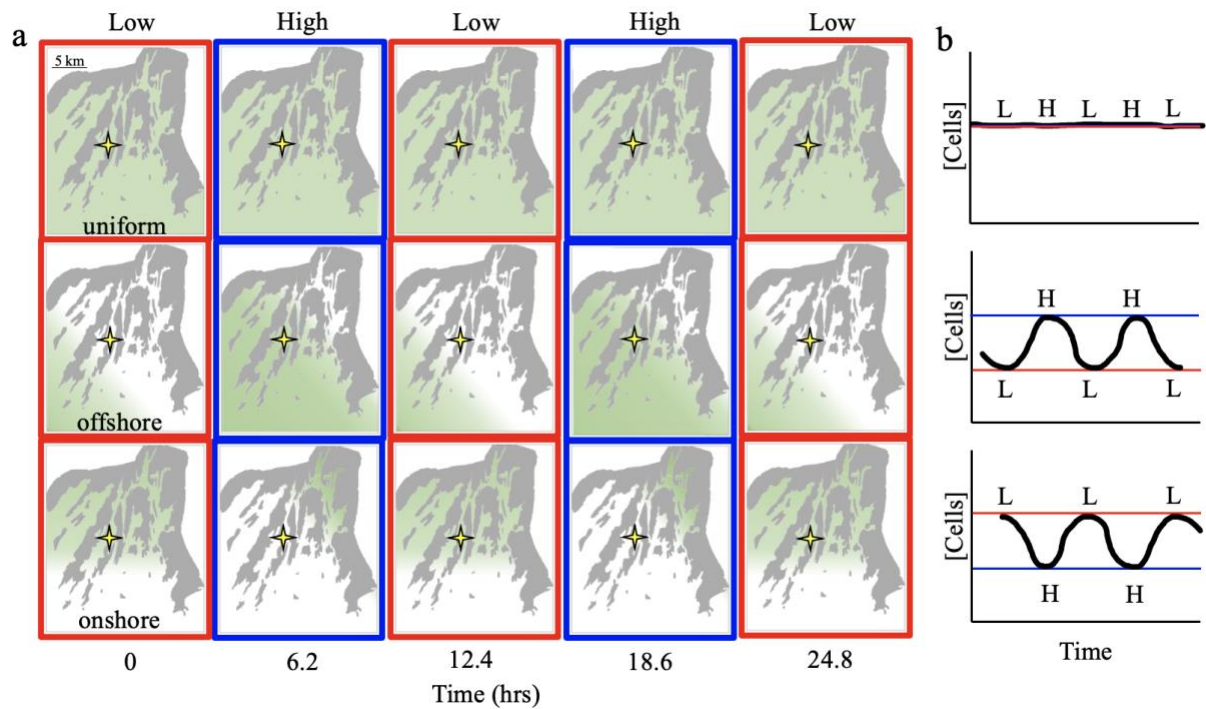


Figure 7. Harpswell Sound spatial patterns (a) and corresponding timeseries (b) that model the tidal advection of a spatially uniform diatom population (represented by the green background color; top row), a population concentrated offshore (middle row), and a population concentrated onshore (bottom row) over two tidal cycles. The star on all maps is the location of the Schiller Coastal Studies Center (SCSC).

The third hypothesis addresses bloom origin. H3a: *Harpswell Sound, being a well-mixed coastal environment, has diatom populations that are uniformly distributed across space and will therefore exhibit no variability in concentration at the tidal cycle frequency.* H3b: *HS is seeded by robust seasonal diatom blooms detected in the GOM and thus shows greater high-tide diatom concentrations at the sampling location in spring and fall.* H3c: *The shallow coves of HS, being well-lit and well-mixed, act as incubators for diatom blooms and therefore show greater low-tide populations at the sampling location, regardless of seasonal physical changes to water column stability.*

### *3.4 Changing composition of toxic blooms in Harpswell Sound*

The fourth hypothesis addresses toxic algae. H4a: *Alexandrium is the most concentrated toxic phytoplankton in HS, given that HS shellfish become toxic due to this taxon on a near-yearly basis and that this taxon is thought to be indigenous to HS (Bean et al. 2005).* H4b: *Low-nutrient summer conditions facilitate toxic blooms in HS, with some blooms occurring earlier given that HS has previously been the first area along the coast of Maine that shows toxicity (Bean et al. 2005).*

## **4 Methods**

### *4.1 Sites, Platforms, and Time Intervals*

The sampling sites in HS were the dock at the Schiller Coastal Studies Center (SCSC; 43°47'31.7"N 69°57'28.6"W) and the location of the Bowdoin Land Ocean Biogeochemical Observatory (LOBO; 43°46'04.5"N 69°59'10.9"W; Figure 8). Platforms used were the flowing seawater lab at the SCSC and a mooring that houses the LOBO. The SCSC marine lab is continuously fed by seawater pumped from Harpswell Sound. The intake pipe is 1.5 m above sea bottom and is situated 8 to 45 m off the coast and in a 3.5 to 7 m water column depending on the tide phase. The LOBO is located 4.4 km southwest of the SCSC, in central Harpswell Sound at a bathymetric slope from shallow to deeper water. Phytoplankton data were collected from 2020 until 2022. Currents, temperature, and salinity data were recorded from 2014 to 2022.

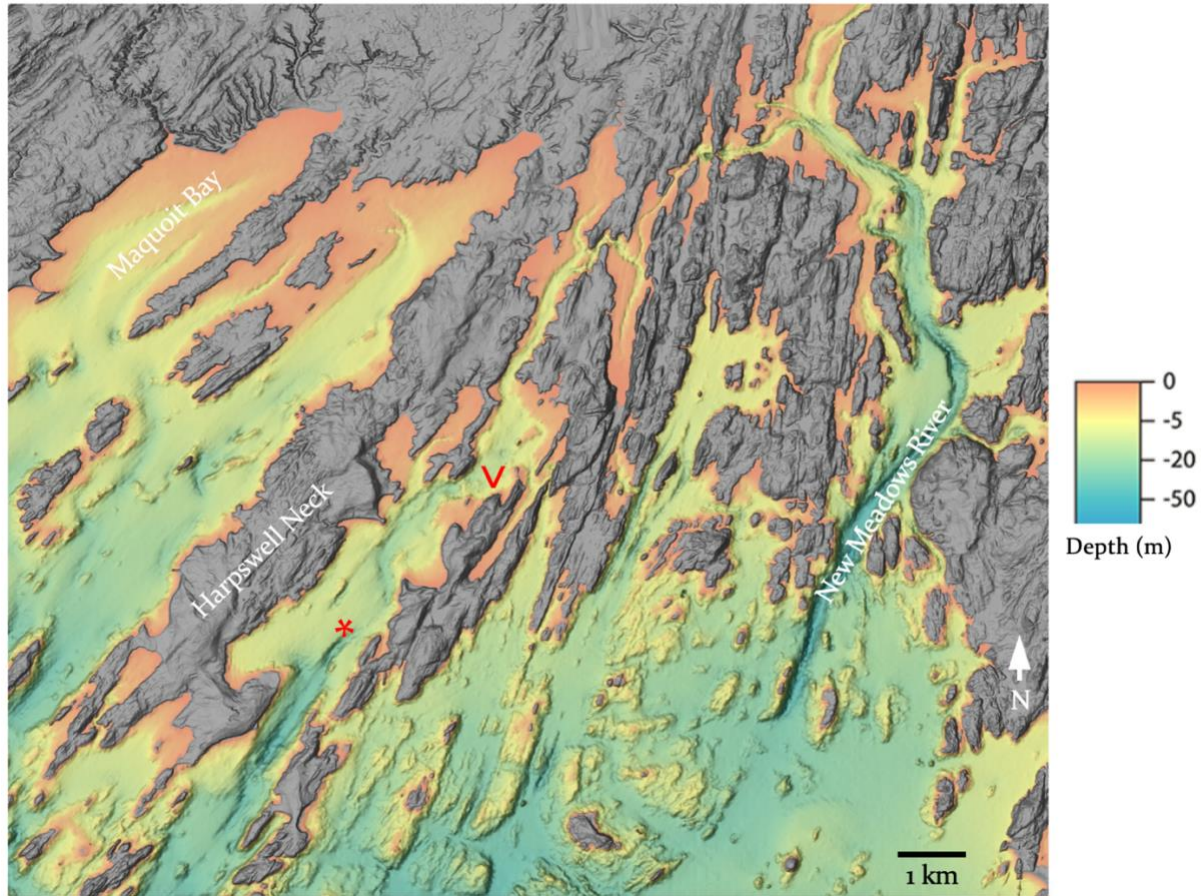


Figure 8. A bathymetric and elevation map of northeastern Casco bay and Harpswell Sound, a 20km-long estuary. An IFCB quantified the phytoplankton community in Harpswell Sound at the Schiller Coastal Studies Center (v symbol) and the Bowdoin Land Ocean Biogeochemical Observatory (\* symbol) collected current velocities, temperature, and salinity. Figure is adapted from the National Centers for Environmental Information (NCEI) DEM Global Mosaic.

#### 4.2 Data and Instrumentation

The data used here are a highly resolved time series in HS of phytoplankton taxonomy from imaging-in-flow cytometry obtained at the flowing seawater lab at SCSC, hydrographic properties of surface temperature and salinity from a mooring, and depth profiles of current velocities from a mooring. All raw phytoplankton images and automated classification files are publicly available (<https://habon-ifcb.whoi.edu/timeline?dataset=harpowell>) and all raw currents, temperature, and salinity data are publicly available (<http://bowdoin.loboviz.com>). MATLAB

R2022A was used to process and graph data. Code and processed data files are publicly available (<https://github.com/cobrien-9/harpswell-sound-plankton-2023>). Code to aid formatting of graphs was obtained on the MATLAB Central File Exchange (Martínez-Cagigal 2023; D'errico 2023).

Digital images of phytoplankton were collected with a McLane Imaging FlowCytobot (IFCB). This imaging-in-flow cytometer collects and analyzes a sample approximately every 25 minutes (Figure 9a). Particles are aligned in a sheath fluid in single file through an interrogation region where a laser triggers fluorescence by chlorophyll (Figure 9b), in turn triggering a camera (Figure 9c) to capture images of all phytoplankton cells (Figure 9d). A neural network-based algorithm (Sosik and Olson 2007; Figure 9e) is the basis for automated classification of cells in the size range of 5  $\mu\text{m}$  and 200  $\mu\text{m}$ , the size range of diatoms (Olson and Sosik 2007; Madin 2005). The classifier output is a value of 0 to 1 representing the probability that the image falls into each of 97 particle categories. The automated classifier was modified by M. Brosnahan to distinguish taxa commonly found in the GOM (personal communication). Taxonomic resolution for living cells ranges from class to species. Cell counts for each taxonomic group were computed by adding the probabilities that each image pertained to each category. The calculated sum of particles in each classification category was divided by the unique sea water sample volume, which ranged from 2.5-4.5 ml depending on particle concentration, to calculate a concentration in cells per ml (Figure 9f).

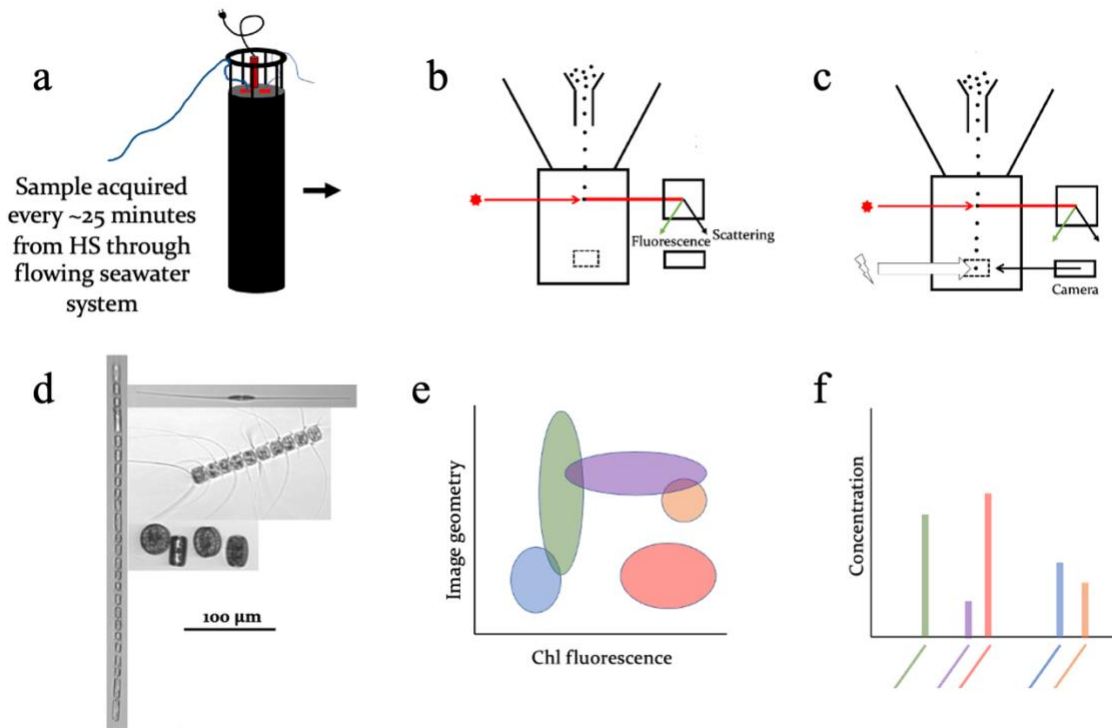


Figure 9. Visual representation of phytoplankton data collection method and Imaging FlowCytobot (IFCB) function. The IFCB (a) collects a sample from the flowing seawater intake connected to HS. Particles are aligned in a sheath fluid to encounter a laser and trigger fluorescence if there is chlorophyll in the particle (b). The fluorescence triggers a camera to capture an image of the particle (c). The images (d) are run through a neural network to predict the probable classification of the particle based on particle geometry and fluorescence (e). The probabilities that each particle pertains to a classification is converted to a cell concentration (f). (b and c are adapted from McLane 2020.)

Hourly timeseries of hydrographic properties were collected on the LOBO mooring. Temperature and salinity were collected with a Sea-Bird Electronics 32 CTD at 1 m depth. A profile of current velocity resolved to 1 m depth intervals was collected with a Teledyne RDI Workhorse Acoustic Doppler Current Profiler (ADCP).

#### 4.3 Data Analysis

The taxa chosen for analysis were *Thalassiosira*, *Chaetoceros*, *Guinardia delicatula*, *Cerataulina pelagica*, *Bacillariophyceae*, and the toxic diatom *Pseudonitzschia* (see Figure 2 for taxa images). These taxa were chosen based on the most imaged diatom taxa from January 2020 to May 2022, which, listed in greatest to least order, were: *Skeletonema*, *Guinardia delicatula*,

*Thalassiosira*, *Chaetoceros*, *Leptocylindrus*, Bacillariophyceae (unidentified pennate), *Cylindrotheca*, *Pseudonitzschia*, pennate, *Dactyliosolen fragilissimus*, and *Cerataulina pelagica* (Figure 10).

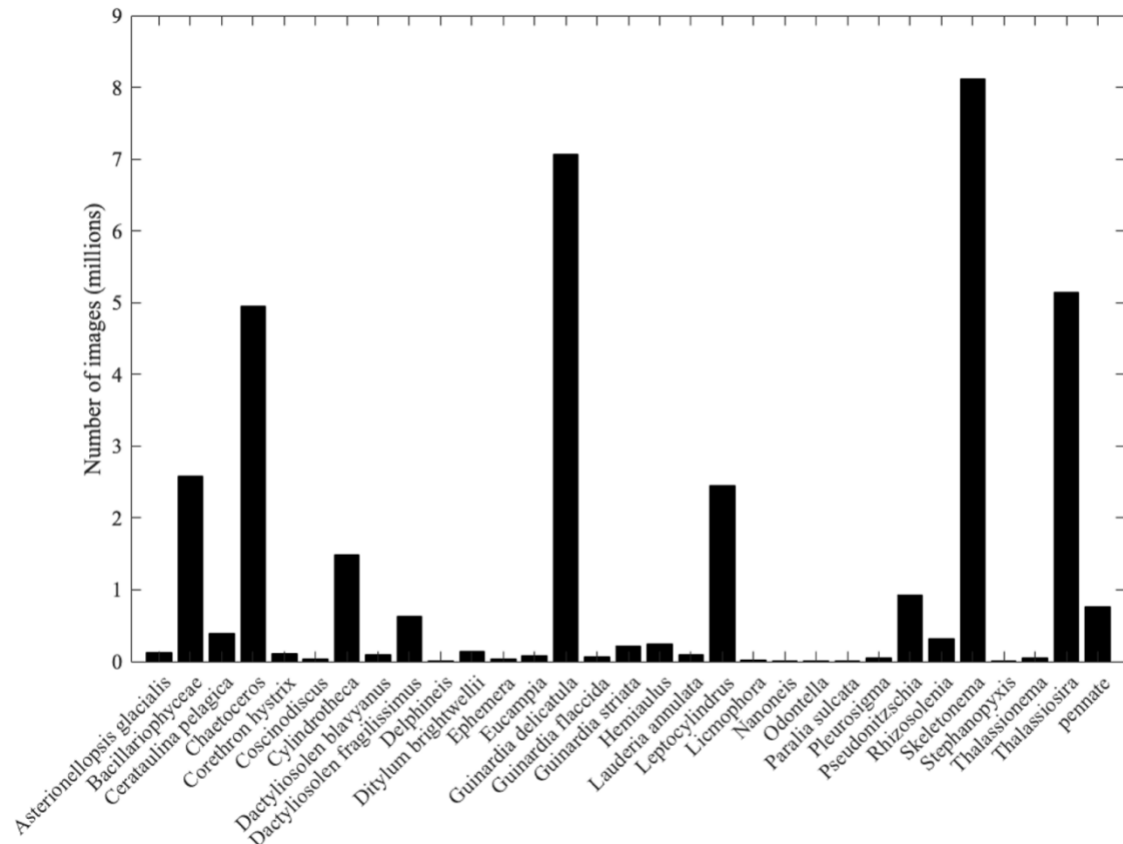


Figure 10. Total image counts from the automated classifier for diatom taxa observed at Schiller Coastal Studies Center, Harpswell Sound, between January 2020 and May 2022.

Representative cell-specific biovolumes for each taxon were acquired using the annotated plankton dataset published by Sosik (2014). The representative biovolumes for major contributors to biovolume use three cells for *Thalassiosira*, *Chaetoceros*, *Guinardia delicatula* and six cells for Unidentified pennates and *Cerataulina pelagica*, (Table 1). Taxon cell concentration was multiplied by its representative image biovolume estimate to compute biovolume concentration ( $\text{cm}^3$  of biovolume per  $\text{m}^3$  of sea water). The representative biovolume

for a taxon is a constant that does not reflect the varying biovolume of the distinct imaged cells. To account for the uncertainty in estimating cell biovolume, figures may include  $\pm 50\%$  error envelopes for each taxon biovolume.

*Table 1. Diatom taxa that were major contributors to biovolume and the metrics used to convert images to biovolume in this study. (Biovolume data for representative images is adapted from Sosik (2014)) The "first occurrence in bloom" counts measure the first taxa to reach peak biovolume in each of 17 blooms identified in the total diatom biovolume timeseries.*

Taxa	Morphology	Representative image biovolume ( $10^3 \mu\text{m}^3$ )	Number of chained cells in representative image	First occurrence in bloom				
				2020	2021	2022	total	% total
Cerataulina pelagica	Centric	341.158	6	0	0	0	0	0
Chaetoceros	Centric	256.5	3	0	1	0	1	5
Guinardia delicatula	Centric	488.572	3	1	1	2	4	24
Pseudonitzschia	Pennate	193.103	3	NA	NA	NA	NA	NA
Unidentified pennate	Pennate	622	6	3	0	0	3	18
Thalassiosira	Centric	515	3	3	5	1	9	53

Spectral analysis using the fast Fourier transform function identified high-frequency cycling in the biovolume of many taxa. The periods for dominant cycles were 12 hours 25 minutes and 24 hours, which correspond to the length of the tidal cycle and of the day, respectively. To create a smoothed daily average of biovolume of each taxon, the tidal cycle and daily cycle (net production-grazing cycle) were removed from the timeseries by calculating a running average of taxon biovolume over a 25-hour moving window, following the approach of Carberry et al. (2019). To separate the tidal endmember biovolumes, times at which LOBO current velocity along the sound equaled zero were used as an indicator of when high tides and low tides occurred. The biovolume of each taxon at those indicated times were interpolated to create separate tidal endmember biovolume timeseries.

The ADCP timeseries from LOBO was processed to calculate the along-sound velocity of currents and remove a strong tidal cycle. The current velocity resolved to 1 m depth intervals was shifted  $45^\circ$  from the north-south-east-west axis to calculate the along-sound and across-sound velocities, following the approach of Peabody (2014). The ADCP resolved current velocity up to

30 m depth. A running average of the along-sound current velocity was calculated over a 25-hour moving window on the raw timeseries (Figure 11a) to remove the tidal cycle as best as possible and resolve the residual current flows (Figure 11b). Peabody (2014) used a similar approach because they found that accounting for all tidal harmonic constituents (more than 20) is computationally intensive and differs insignificantly in accuracy. Outlier residual velocity values ( $>100$  cm/s), most of which occurred below 28 m due to contact with sea bottom or suspended sediment, were removed.

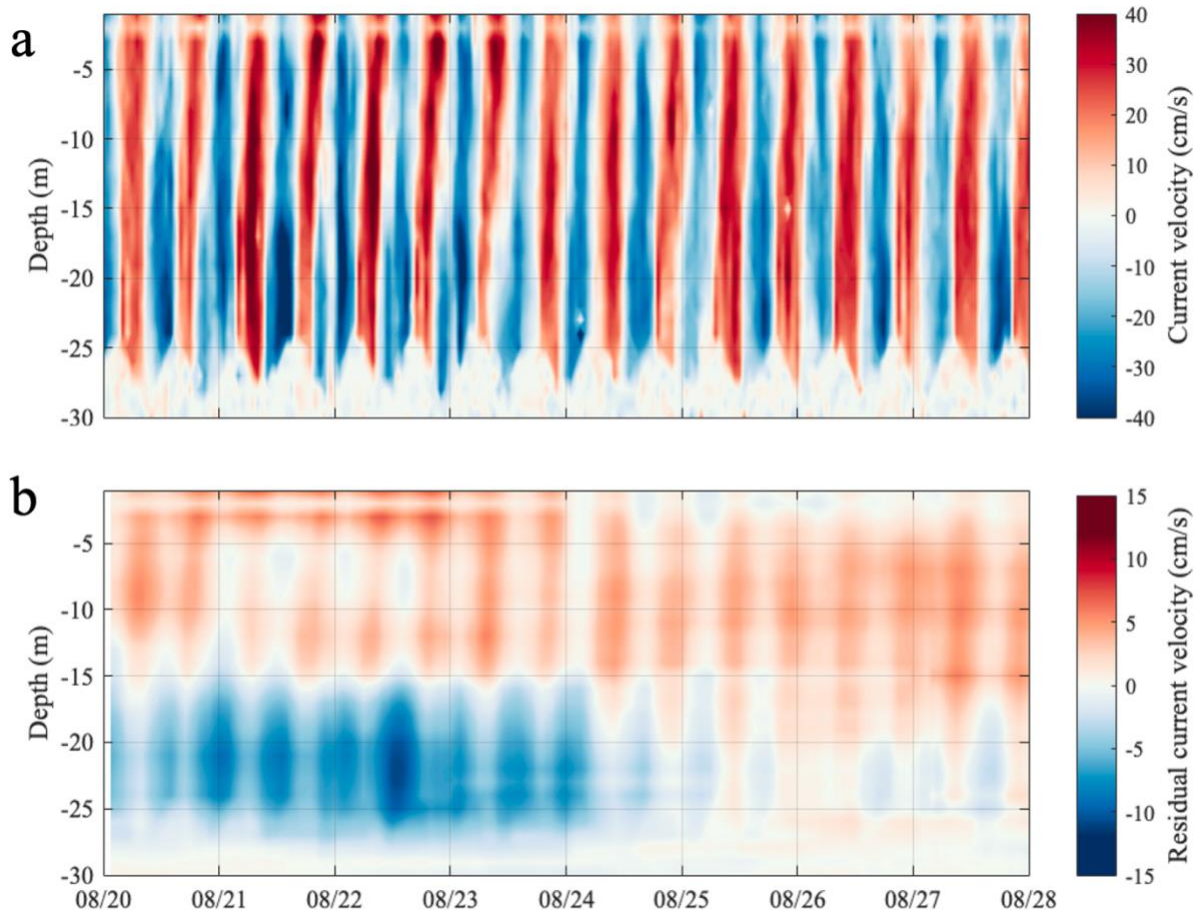


Figure 11. Along-sound current velocity profiles at the LOBO mooring during a week in August 2021: the raw tidal timeseries (a) and the smoothed 25-hour moving average timeseries (b). Positive values indicate flow into the sound and negative values indicate flow out of the sound. Note the different color bar scales between (a) and (b).

## 5 Results

### 5.1 Seasonal blooms

Hydrographic data from 2014 to 2022 in HS exhibit strong seasonality. Surface water temperature in HS consistently oscillated from coldest values in February to warmest values in July or August, with a corresponding range from 0 °C to 22 °C (Figure 12a). Surface salinity had interannual variability with a range of 22 ppt to 32.5 ppt (Figure 12b). Week- to month-long excursions below 28 ppt most often occurred in April and May. Salinity observations remained above 30 ppt in December, January, and February.

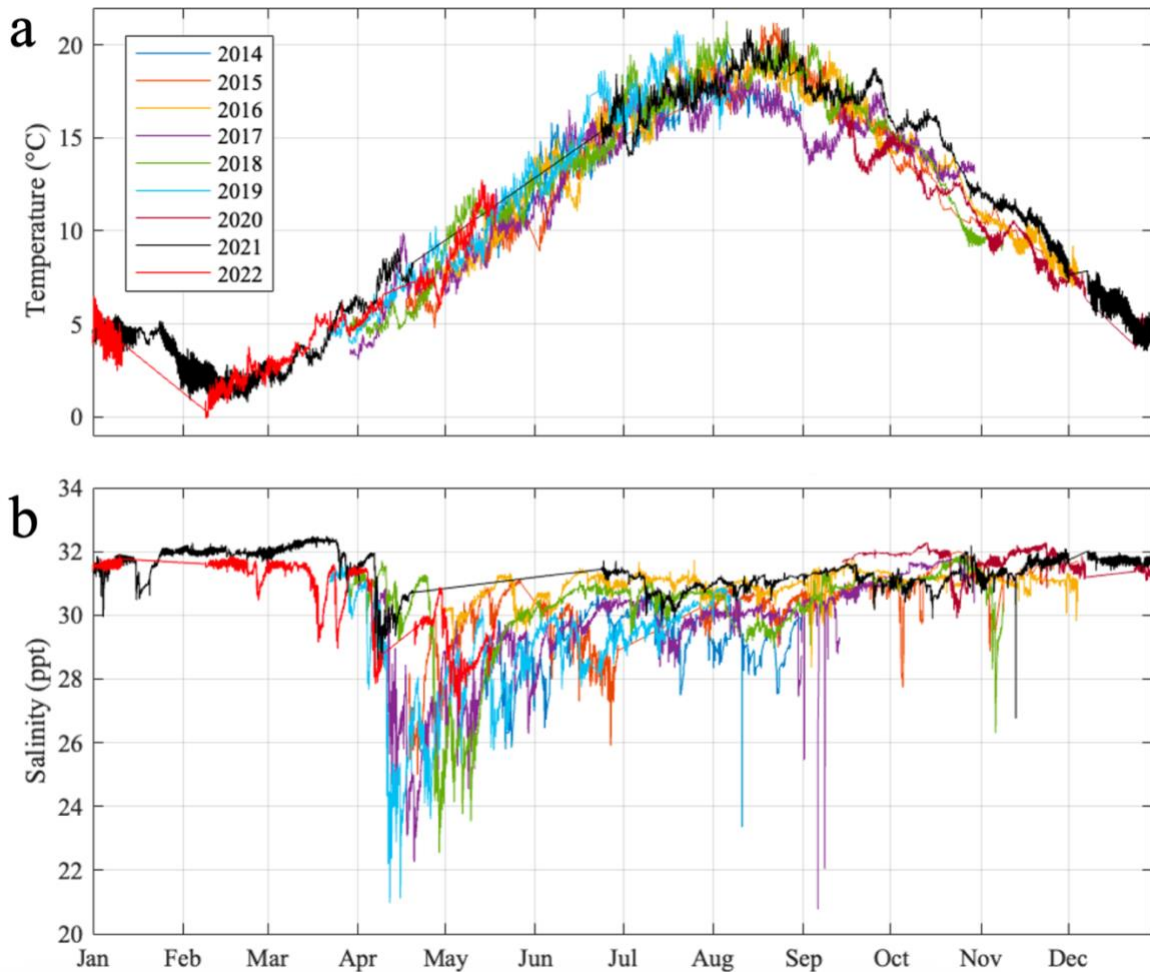


Figure 12. Hourly observations of temperature (a) and salinity (b) at 1 m depth at the LOBO mooring made between 2014 and 2022 (color refers to year;  $n=53,715$ ).

When the mixed semi-diurnal tidal velocity is removed to reveal the residual velocity (Figure 11), HS appears to have distinct seasonal circulation regimes based on the 2014-2022 current profile timeseries. In May through September, the residual current velocities below 15m were mostly out of HS and into HS above 10 m (Figure 13 a, b, c). Residual current velocities were mostly homogenous below 5m between October and April (Figure 13 d, e), during which the strongest currents were observed in pulses of water into HS below 5 m. The surface (above 2 m depth) residual current in these cold months was slightly out of HS most of the time.

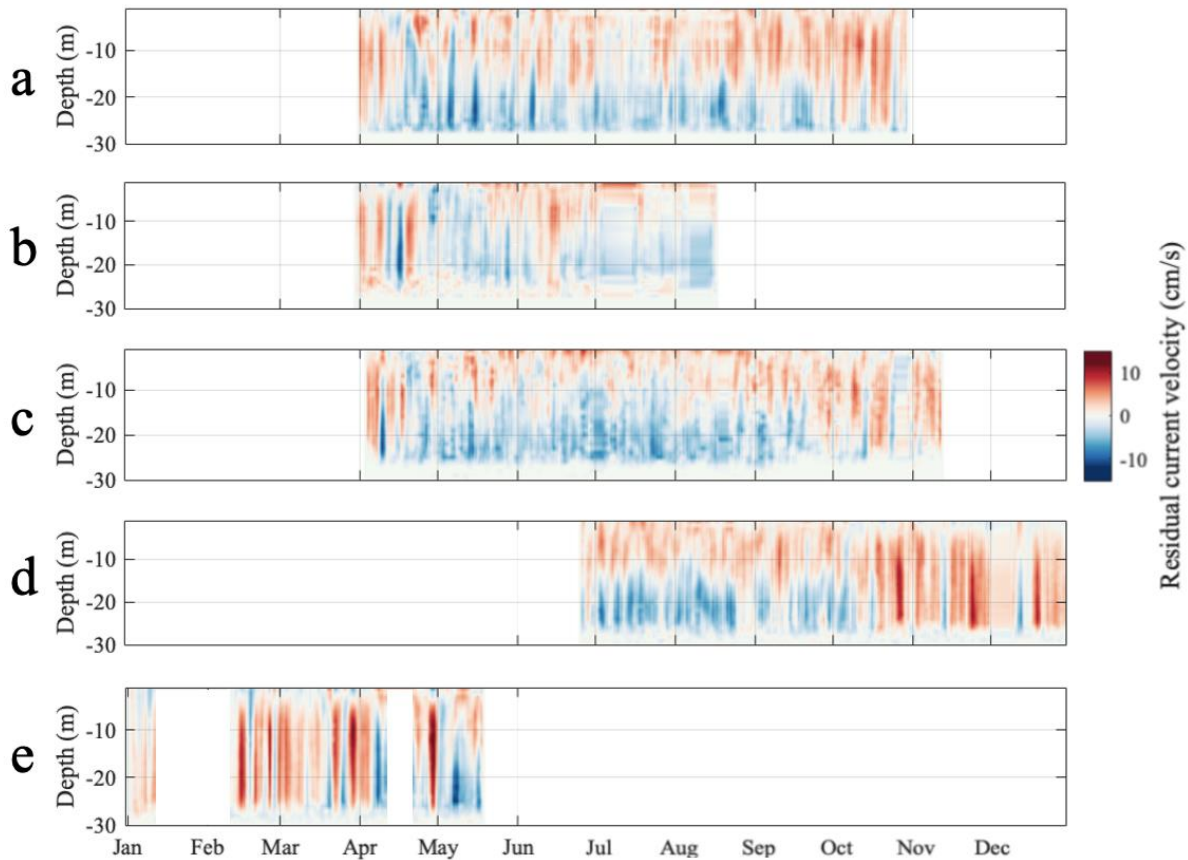


Figure 13. Along-sound residual current velocity profiles at the LOBO mooring in 2017 (a), 2018 (b), 2019 (c), 2021 (d), and 2022 (e). Positive values indicate flow into the sound and negative values indicate flow out of the sound.

A seasonal pattern of circulation in HS was observed by coupling residual current velocities with water properties. Residual surface flow into HS most likely occurred in spring and summer with warming water and the freshest water (Figure 14). Residual surface outflow most likely occurred in late fall through winter; this water was cooling and higher in salinity. Spring is most variable in both residual inflow/outflow velocity and salinity as a result of the strengthened Kennebec River bloom, presumably during snow melt and spring rains.

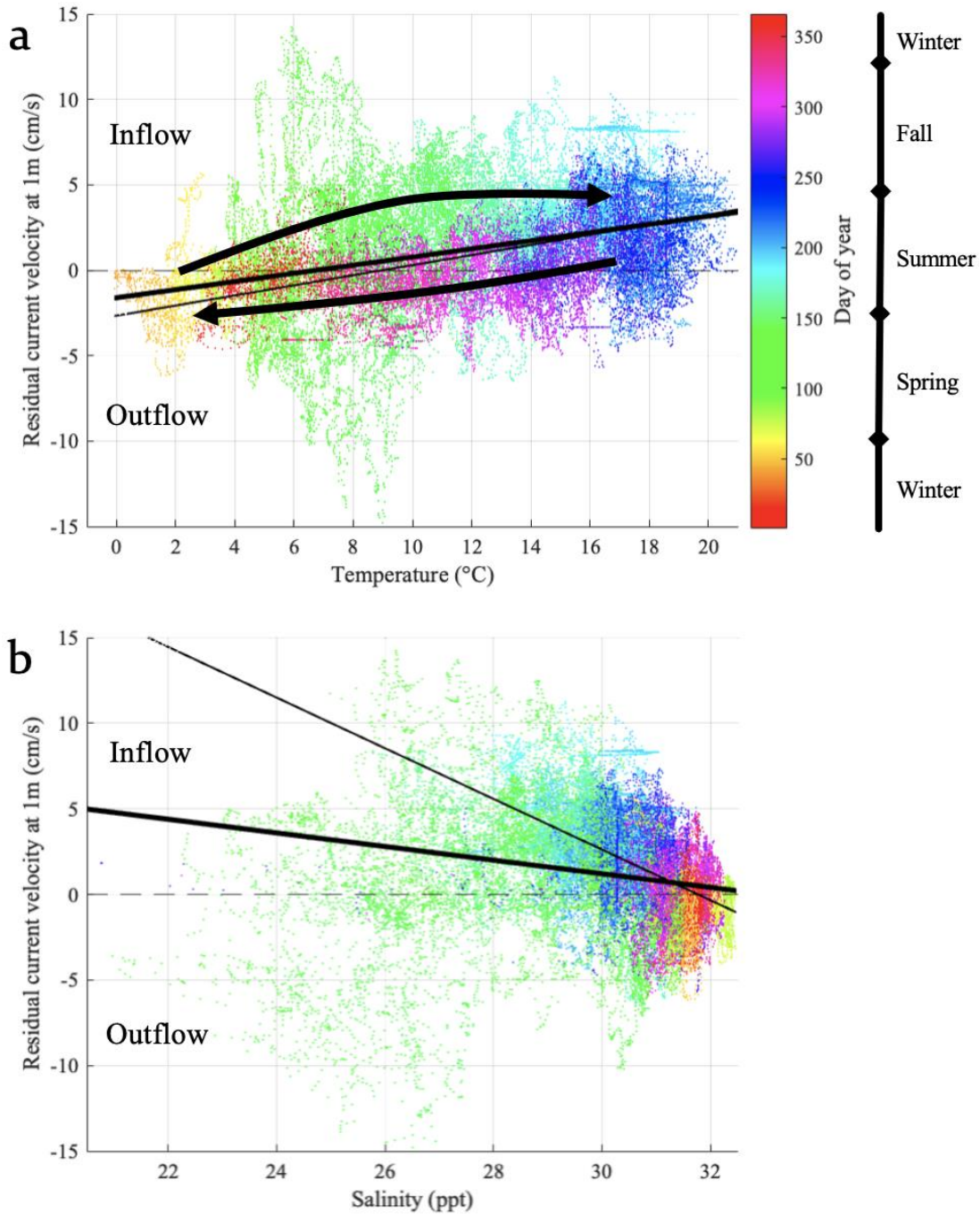


Figure 14. Hourly observations of residual current velocity versus temperature (a) and salinity (b) at 1 m depth at LOBO between 2014 and 2022 ( $n=53,715$ ; colorbar indicates day of year). A positive residual current represents flow into the sound and negative values signify flow out of the sound. Thick lines are best fit for data (salinity:  $y=-0.40x+13.14$ ,  $R^2=0.03$ ; temperature:  $y=0.24x-1.61$ ,  $R^2=0.13$ ). Note the large variability of residual current velocity in spring (green dots). Thin lines represent the best fit of data with April and May data removed (salinity:  $y=-1.48x+47.00$ ,  $R^2=0.23$ ; temperature:  $y=0.29x-2.66$ ,  $R^2=0.23$ ).

The concentration of nutrients in HS between 2020 and 2021 had an observable seasonal pattern but showed interannual variability. The highest concentrations of nitrate and silicate at any depth tended to occur in late fall, winter, and early spring (Figure 15). Anomalously high nitrate was observed at all depths in January of 2021 and anomalously high silicate was observed first at the surface then at depth in April and May of 2022. The highest phosphate levels were recorded May through October, with anomalously high values at the surface in July 2021 and at 5 m in December 2021. Nitrate and silicate are limited in spring and summer, and phosphate is limited in winter.

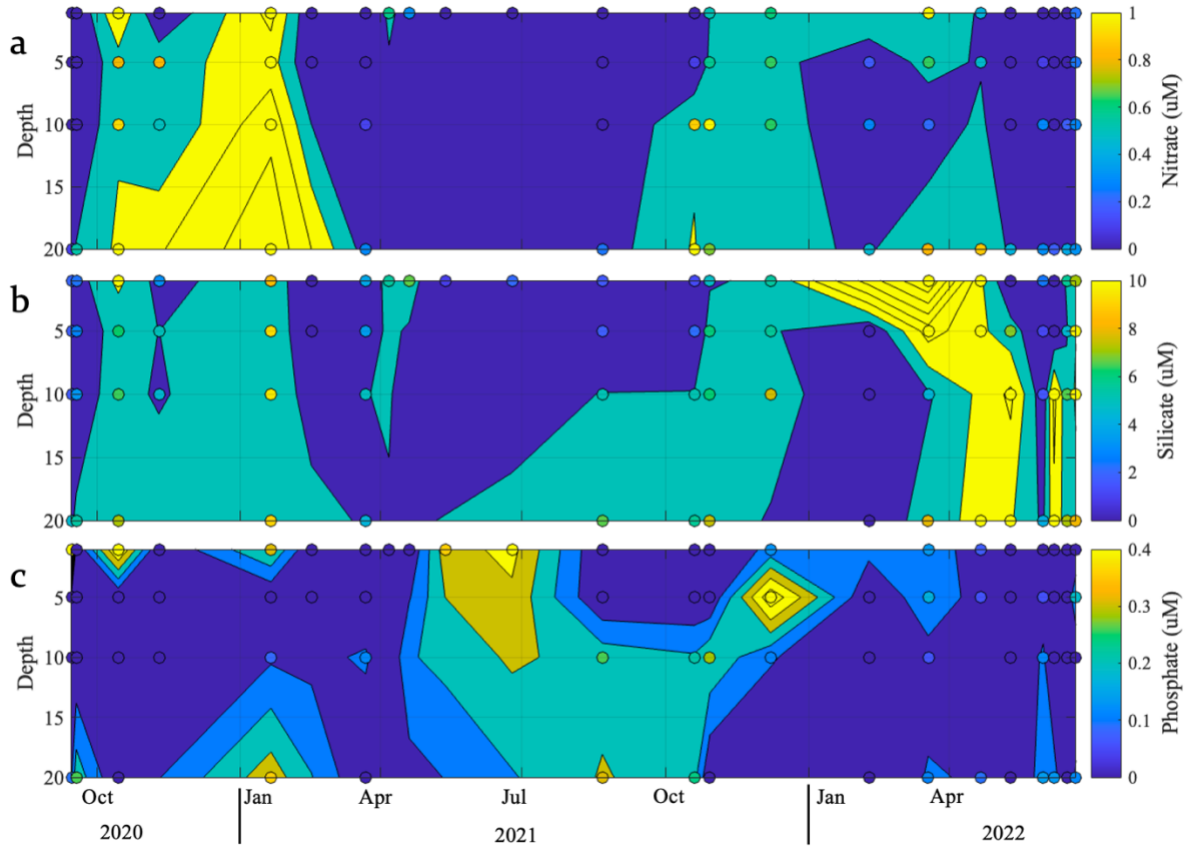


Figure 15. Timeseries profiles of nitrate (a), silicate (b), and phosphate (c) concentration measured at four depths at the LOBO mooring. Note different colorbar scales between (a), (b), and (c), in units of  $\mu\text{M}$ . Figure courtesy of Lyle Altschul.

Almost three years of data begin to characterize if seasonal diatom blooms take place. The diatom biovolume maximum was  $489 \text{ cm}^3/\text{m}^3$ . Blooms exceeding  $400 \text{ cm}^3/\text{m}^3$  were observed in March-April and August-September (Figure 16). Shorter duration diatom blooms of less than  $100 \text{ cm}^3/\text{m}^3$  were in all months, but the months with the smallest diatom biovolume were May and October. A 5-month sustained increase in diatom biovolume began developing in November of 2021 (Figure 16 b, c).

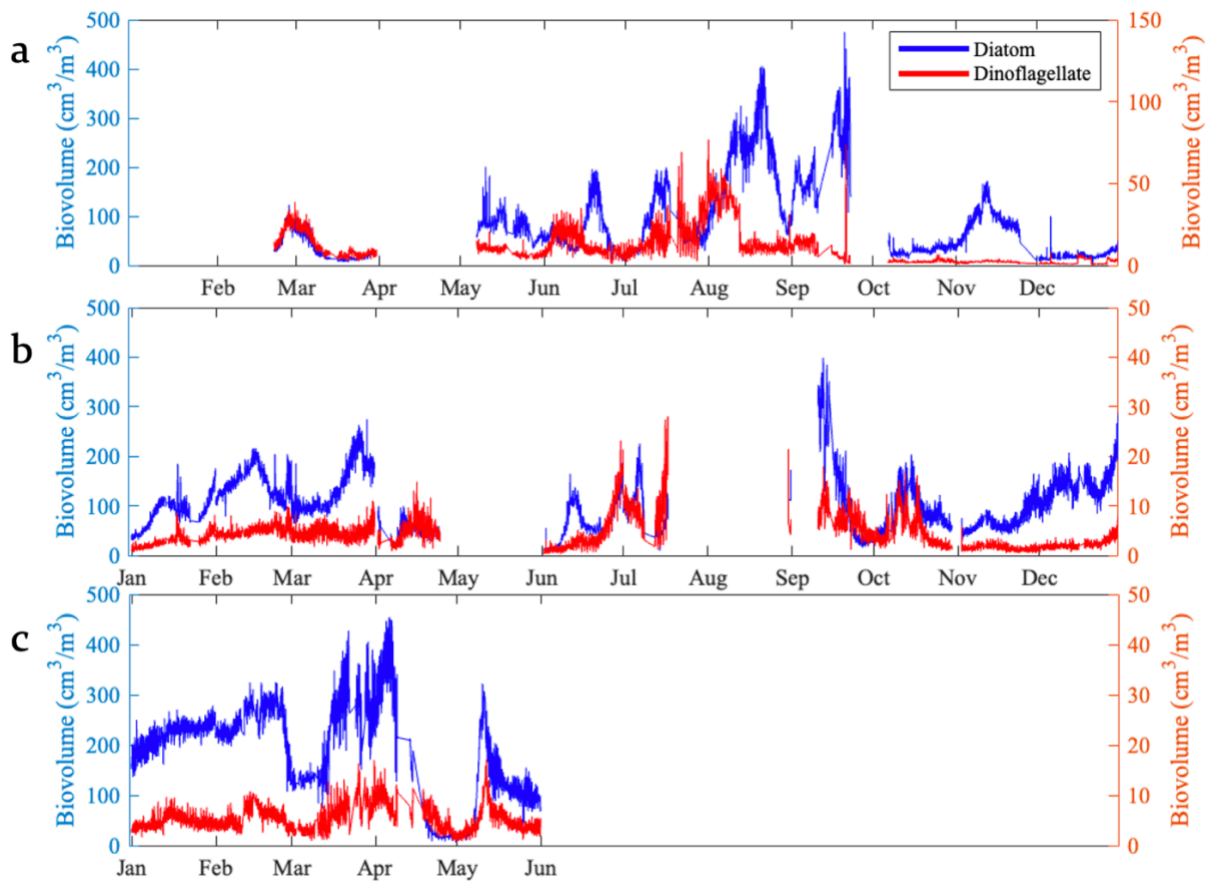


Figure 16. Raw biovolume observations from SCSC at half-hour resolution in 2020 (a), 2021 (b), and 2022 (c). The left vertical axis corresponds to diatom biovolume (blue) and the right vertical axis corresponds to dinoflagellate biovolume (red). Note the different vertical axis scales for diatoms and dinoflagellates between (a) and (b) & (c) for dinoflagellates.

## 5.2 Successional patterns

Dinoflagellates were observed to bloom during diatom blooms and between diatom blooms. Dinoflagellate biovolume was a factor of three to ten lower than diatom biovolume (Figure 16; see Figure S2 for exceptional intervals in which diatom and dinoflagellate biovolume were equal). Dinoflagellates did not exhibit strong blooms in spring and fall like diatoms, but rather the greatest dinoflagellate biovolume was observed in the summer after diatom blooms with the peak dinoflagellate biovolume occurring five to ten days after the peak diatom biovolume. December through April, the pattern of dinoflagellate biovolume was synchronous with diatom biovolume.

Thirty-one diatom taxa are classified in the automated classifier, but the taxa that contribute most to the total diatom biovolume are *Thalassiosira*, *Chaetoceros*, *Guinardia delicatula*, unidentified pennates, and *Cerataulina pelagica*. Each of the diatom blooms observed in Figure 16 are composed of varying proportions of these five major groups (Figure 17). Generally, *Thalassiosira* achieved peak biovolume first in the bloom sequences in May, August, and September 2020; January, April, June, and October 2021; and May 2022. *Guinardia delicatula* was first to peak in bloom sequences in June 2020, March 2021, and February and March 2022. *Chaetoceros* was first to peak in the bloom sequence of January 2021. Unidentified pennates were first to peak in bloom sequences in February, August, and November of 2020. *Cerataulina pelagica* does not appear to peak first in any bloom sequences. *Guinardia delicatula* and *Thalassiosira* were most likely to reach their peak biovolume first in the bloom sequences of taxa observed: *Guinardia delicatula* peaked first in 24% of blooms observed and *Thalassiosira* peaked first in 53% of blooms observed (Table 1).

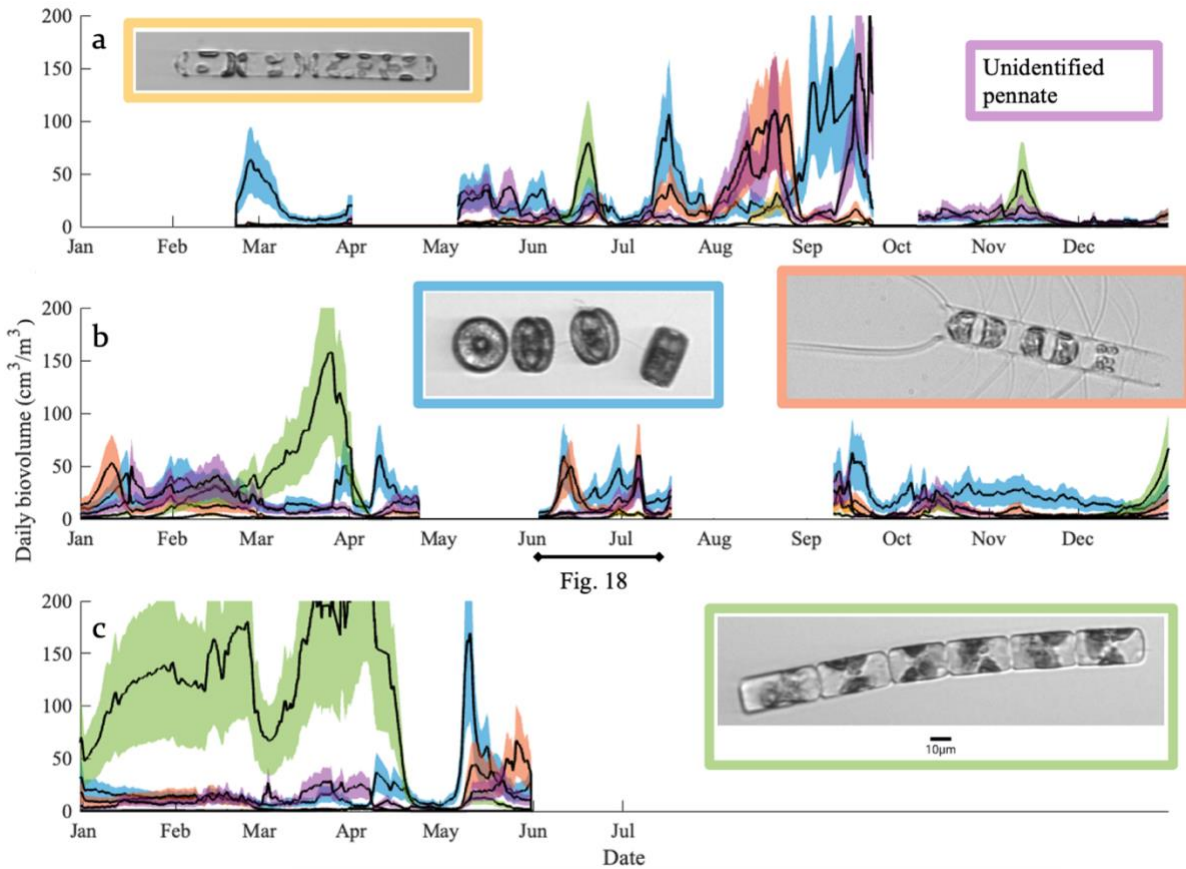


Figure 17. Smoothed timeseries of daily biovolume of diatom groups that most contributed to blooms in 2020 (a), 2021 (b), and 2022 (c). *Cerataulina pelagica*: yellow, unidentified pennate: purple, *Thalassiosira*: blue, *Chaetoceros*: orange, *Guinardia delicatula*: green.

The duration bloom onset to peak biovolume varied within each year and across years. Blooms developed over a few days in the summer and over a few weeks in spring and fall. The exception is the *Guinardia delicatula* bloom development from December 2021 through March 2022. This temporal scale of development contrasts the bloom of the same taxa in the year before (2021), which was less voluminous and underwent most of its growth in February and March.

### 5.3 Origin of diatom blooms

Observations of taxa on interannual time scales obscures how those taxa are distributed in the estuary. Exploring the blooms of taxa on finer temporal scales reveals significant differences in concentrations between adjacent slack tides (high vs. low). An example of such occurred in

June 2021 (Figure 18). During this interval, *Cerataulina pelagica* exhibited three blooms with decreasing biovolume, with a maximum of  $13 \text{ cm}^3/\text{m}^3$ . The biovolume concentration did not vary with tide phase throughout the time interval, indicating uniform spatial distribution (Figure 18a). In contrast, *Chaetoceros* bloomed before the first *Cerataulina* bloom and at the same time as the third bloom. The maximum biovolume was about  $64 \text{ cm}^3/\text{m}^3$ . During the first bloom, the high tide population biovolume was greater than the low tide population biovolume by nearly a factor of two, while they were similar in the last bloom (Figure 18b). This indicates that the first bloom originated offshore, while the last bloom was uniform across the estuary. Finally, *Thalassiosira* bloomed nearly synchronous with the first *Chaetoceros* bloom to a biovolume of  $104 \text{ cm}^3/\text{m}^3$ . The low tide population biovolume was greater than the high tide population biovolume by a factor of 2.8 at the bloom peak (Figure 18c), indicating the bloom initiated upstream in HS. The last two blooms were synchronous with *Cerataulina* and the last with *Chaetoceros*, all with uniform concentrations across the estuary. This example indicates that specific taxa can originate in different locations but at the same time or multiple taxa can bloom in the same space and at the same time.

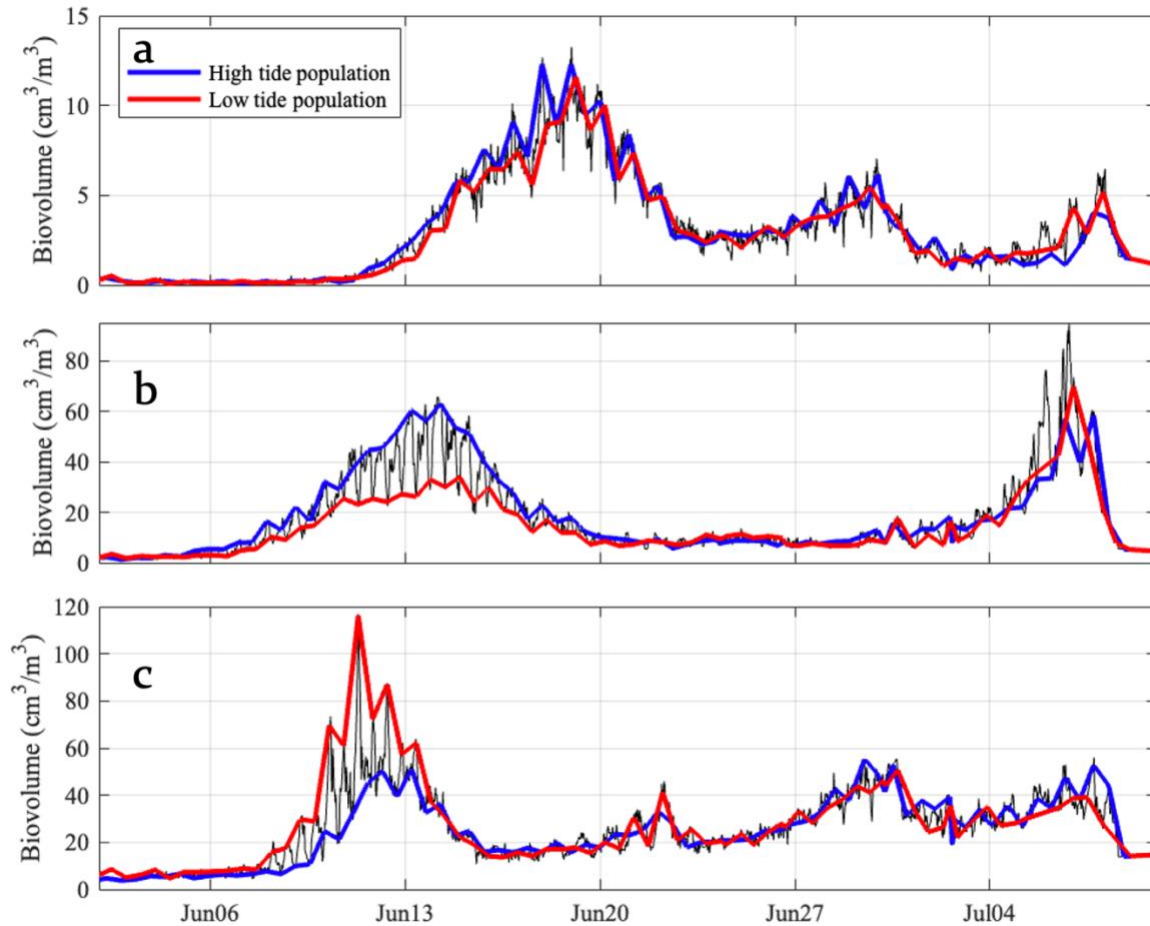


Figure 18. Biovolume timeseries of *Cerataulina pelagica* (a), *Chaetoceros* (b), and *Thalassiosira* (c) in June and July of 2021. High tide (blue) and low tide (red) population concentrations evidence origin of the bloom. Note the different vertical axis scales for (a), (b), and (c).

The most unexpected bloom was also the largest biovolume of a diatom species, reached on April 5th, 2022, by *Guinardia delicatula* after slow extended growth of five months. The spatial partitioning of the population varied during a dynamic spring physical context.

Temperature steadily declined through December and early January except for a local peak on January 1st (Figure 19a), which coincided with the transition of the residual current regime from flow out of HS at the surface and flow into HS at depth to flow into HS at the surface and flow out of HS at depth (Figure 19b). This event took place two days after spring tide (Figure 19c).

During this transition the high and low tide biovolume concentrations of both *Guinardia*

*delicatula* and *Pseudonitzschia* were reduced by 20%, which contrasts sustained winter growth before and after the event (Figure 19d). The populations declined by mid-January and sustained their value through the first half of February. Anomalous low salinity and high temperature surface water was observed in the last week of March, at which time there was a current regime switch (the same as observed on January 1st) and a reduction in biovolume from 200 cm<sup>3</sup>/m<sup>3</sup> to 100 cm<sup>3</sup>/m<sup>3</sup>. Similar pulses of surface freshwater flowing into HS were observed March 17th-21st, March 24th-26th, and April 6th-12th. Each pulse of Kennebec River freshwater resulted in a 25% to 50% reduction in the cells in the incoming waters. The timing of biovolume reductions and the size of the reductions did not correlate positively or negatively with tidal magnification over the spring neap cycle.

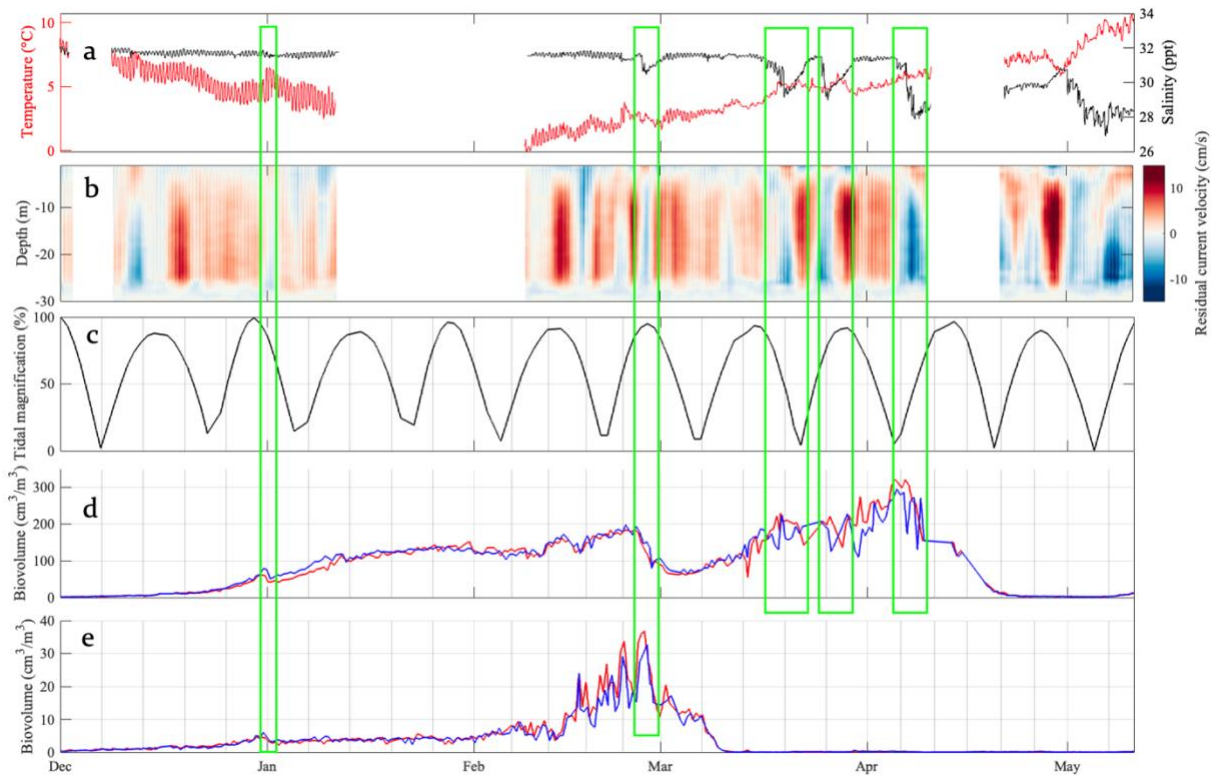


Figure 19. Physical context of a slow-growth diatom bloom and a toxic diatom bloom from December 2021 through April 2022. Temperature and salinity of surface water at the LOBO mooring (a); residual currents at all LOBO mooring depths (b; positive is flow into the sound); tidal magnification in South Harpswell based on lunar illumination and how close the moon is to earth, a proxy for the spring-neap cycle (c); high tide biovolume (blue) and low tide biovolume (red) of *Guinardia delicatula* (d) and of *Pseudonitzschia* (e). Intervals highlighted by green boxes are characterized by anomalous flow of warmer and fresher water into the sound at the surface, and by reduction in *Guinardia delicatula* and *Pseudonitzschia* biovolume. Note different axis scales for (d) and (e).

The *Guinardia delicatula* bloom was slightly larger offshore during early growth, was uniformly distributed in HS for two months, and then mostly concentrated inshore at the bloom peak. From December 31st to January 12th, the high tide population was 21% to 34% larger than the low tide population (Figure 19d), indicating offshore origin. January 13th through March 14th the populations had similar concentrations, but then the tidal endmember biovolumes decoupled for the remainder of the bloom. In late March and Early April, low tide biovolume was up to 59% larger than the high tide, indicating upstream origin.

The largest biovolume of *Pseudonitzschia* was achieved on February 28th, 2022. Biovolume of *Pseudonitzschia* plateaued at 3.7 cm<sup>3</sup>/m<sup>3</sup> through January and early February 2022

(Figure 19e). The biovolume grew from that value to  $34.5 \text{ cm}^3/\text{m}^3$  in three weeks. Within two weeks the biovolume dropped to  $0 \text{ cm}^3/\text{m}^3$ . The high and low tide populations of *Pseudonitzschia* were similar until mid-February, when the population biovolumes decoupled and the low tide population became the most concentrated, indicating origin upstream. Both populations fluctuated five times in late February between  $15$  and  $35 \text{ cm}^3/\text{m}^3$ . The population was most concentrated during these fluctuations when the residual current at the surface was into HS.

#### 5.4 Changing composition of toxic blooms

The classifier does not distinguish at the species level for most groups but does identify dinoflagellate taxa capable of causing HABs (*Alexandrium catenella*, *Dinophysis acuminata*, *Dinophysis norvegica*, *Gonyaulax*, *Karenia*, and *Heterocapsa triquetra*), as well as the diatom genus *Pseudonitzschia*. The combined biovolume of these toxic phytoplankton taxa peaked at the beginning of August 2020 and at the end of February 2022 (Figure 20). *Heterocapsa triquetra* had the largest bloom in 2020 while *Pseudonitzschia* had the largest bloom in 2022. *Heterocapsa triquetra* and *Pseudonitzschia* were the most abundant toxic taxa in 2020, but *Karenia* and *Dinophysis acuminata* were nearly equally abundant as those taxa in 2021. In the first half of 2022, the most abundant taxa were *Pseudonitzschia* and *Dinophysis acuminata*.

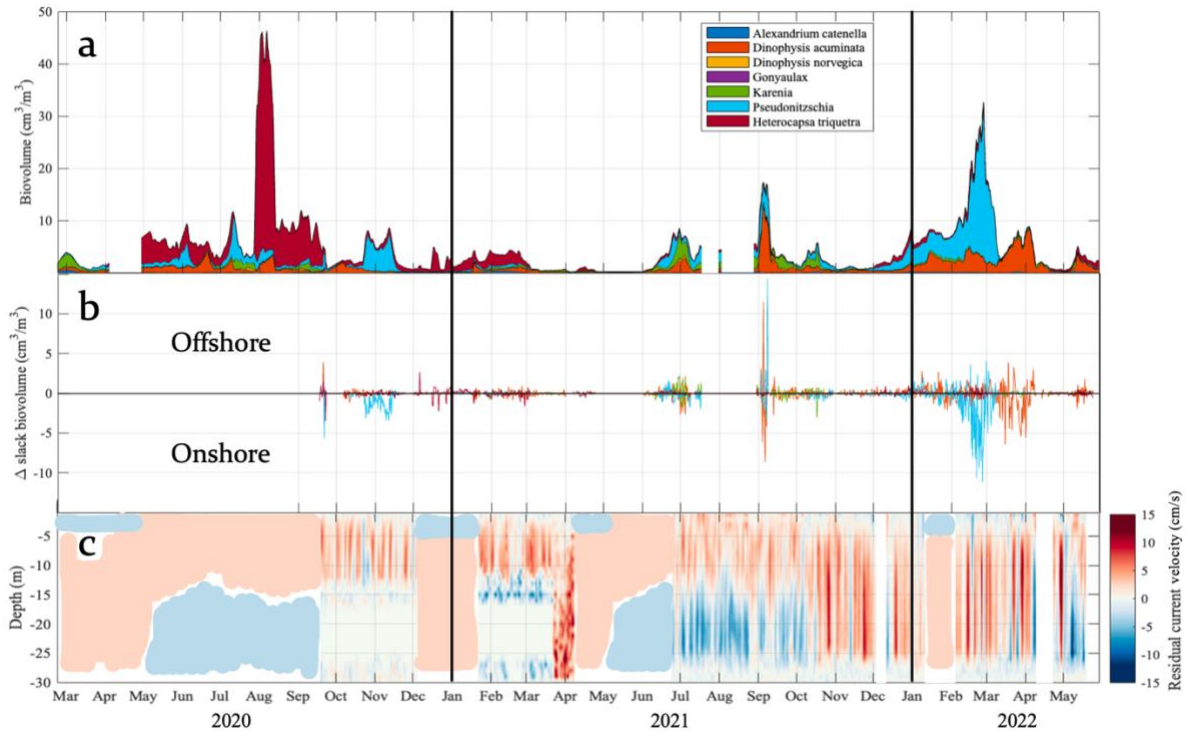


Figure 20. Stacked daily average biovolume of all identified toxic phytoplankton taxa from 2020 to mid-2022 (a). Degree to which each taxon's high tide population is greater than their low tide population (b). Residual currents of all depths at the LOBO mooring, with shaded inferred velocities based on previous years (c; positive indicates inflow).

Toxic dinoflagellates tended to bloom in the summer months when the residual currents flow into HS at the surface and out of HS across a 15m depth boundary, but there were notable exceptions. *Pseudonitzschia* and *Dinophysis acuminata* did not follow this pattern. However, during March 2022, in which there was net inflow below 4m depth, *Dinophysis acuminata* bloomed repeatedly with a low tide population 1 to 5  $\text{cm}^3/\text{m}^3$  greater than the high tide population, which indicates export out of HS could take place. Similarly, larger onshore biovolumes of *Pseudonitzschia* were observed during blooms in October and November of 2020 and in February 2022. The low tide population had a biovolume that was 1 to 12  $\text{cm}^3/\text{m}^3$  greater than the high tide population during the bloom, indicating export was possible. The combined biovolume of taxa that can produce toxins was an order of magnitude larger in February 2022

than in February 2021. There appears to have been a shift from *Heterocapsa triquetra* to *Pseudonitzschia* as the dominant former of blooms.

## 6 Discussion

### 6.1 Seasonal blooms

H1, the hypothesis that HS exhibits a single spring bloom and fall bloom of diatoms, with the magnitude of the spring bloom exceeding that of the fall bloom, is refuted. The driver of the difference in bloom seasonality between HS, the GOM, and the broader North Atlantic is perhaps more frequent mixing in HS by the resident tidal mixing front.

Phytoplankton certainly bloom in the spring and fall in HS, as was predicted by the canonical spring-fall bloom pattern observed in the GOM (Song et al. 2010) and North Atlantic (Martinez et al. 2011). However, smaller, shorter-lived blooms were also observed in every month, in contrast to the model. Diatom blooms in HS were observed in the summer of the 2020 and 2021, although they were often smaller and shorter-lived than other blooms (an exception being August 2020). The spring bloom has the potential to slowly develop during the winter months, exemplified by 2022. A sustained diatom contribution to total phytoplankton biovolume through winter into spring contrasts the distinct phytoplankton community compositions observed between winter and spring in the western North Atlantic (Bolaños et al. 2012). The spring bloom in HS was observed in March and the fall bloom in August and September, when the residual current regime transitioned between a winter upwelling incubation mode and a summer downwelling retention mode (Nardelli & Roesler 2014; Figure 21). Spring and fall had multiple intervals of peak biovolume with different diatom community compositions.

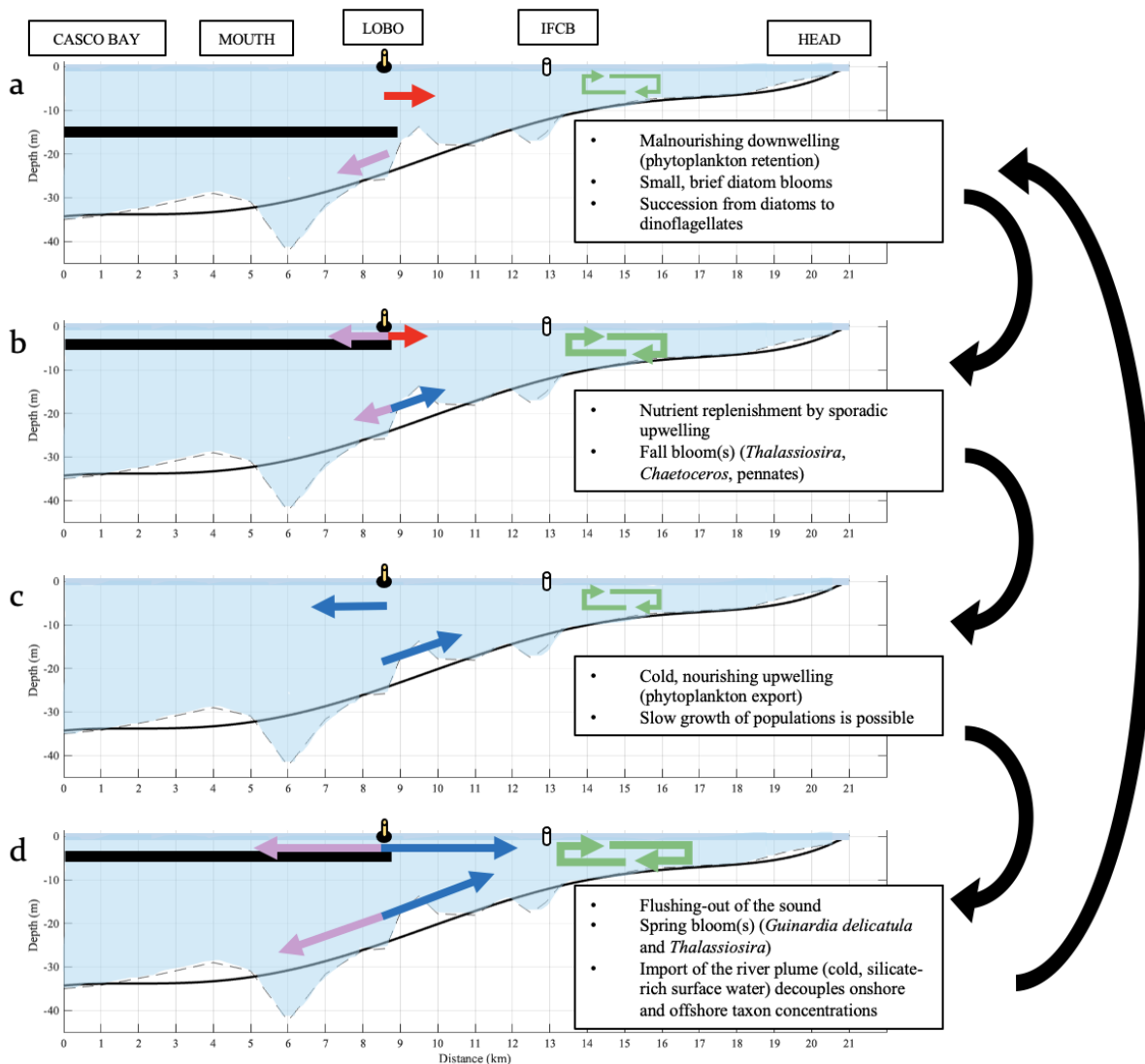


Figure 21. Average residual current patterns coupled with water properties in HS and corresponding phytoplankton bloom dynamics observed in summer (a), fall (b), winter (c), and spring (d). The black horizontal line indicates the depth of the stratification layer. Arrow color symbolizes water temperature anomaly (colder=blue, warmer=red) and arrow length symbolizes the velocity of the average residual current. The bathymetry of HS at its deepest point is shown by the dashed gray curve and a fifth-order polynomial fit of bathymetry is shown by the solid black curve. Bathymetry data is from the NCEI DEM Global Mosaic.

The spring bloom of diatoms appears to be more voluminous than the fall bloom in contrast to the little difference observed between spring and fall bloom sizes in the western North Atlantic in the 1980s and 2000s (Martinez et al. 2011). However, comparison between spring and fall bloom size is limited by the length (2.5 years) and missing data within that interval.

Blooms in spring, fall, and summer consistently accounted for greater than 50% of the total phytoplankton biovolume, contrary to what Bolaños et al. (2012) found in the North Atlantic shelf off the GOM. However, these results were a product of distinct methods. This project underestimated the biovolume contribution of phytoplankton  $<8 \mu\text{m}$  and likely overestimated diatom biovolume by neglecting natural variations in cell size. Thus biovolume becomes more poorly constrained as taxon image counts increased. Resolving individual cell biovolume would reduce the uncertainty of this analysis.

Correlating phytoplankton concentrations with seasonal nutrient concentrations in HS was previously difficult due to limited discrete sampling capacity (Hankinson et al. 2010). The mostly-continuous, highly-resolved phytoplankton biovolume timeseries used in this study makes comparison with nutrients more accurate. A higher local silicate concentration in HS in March of 2022 compared to March of 2021 (Figure 15b) could have fueled the extensive 2022 *Guinardia delicatula* bloom. Despite higher nitrate concentration in January of 2021 compared to January of 2022 (Figure 15a), total dinoflagellate biovolume was unexpectedly less. Because diatoms need both nitrate and silicate, the succession of diatoms to dinoflagellates in summer suggests intervals of replete silicate followed by intervals of silicate limitation. This intermittent source of silicate that triggers small diatom blooms could be the tidal mixing front, mixing during strong winds, or the Kennebec River plume (Ballance 2020).

The spring bloom appears to have a more complex cause than solely the increase in stratification or the surpassing of a temperature threshold that limits growth. The surface water injections of the Kennebec River plume into HS appear to sometimes reduce diatom concentration, but there is no evidence for the mechanism by which they do so (potential causes are dilution of the bloom or of nutrients, subduction under the plume, or high CDOM and light

limitation). To complicate the story, the first pulses of Kennebec River water also appear to increase silicate concentration in HS, which would promote diatom growth. Freshwater injections have a differential impact, or spatially disparate impact, on offshore and onshore diatom communities, but bloom development and decline do not appear to correlate with the spring-neap cycle.

## 6.2 Succession patterns

H2a, the hypothesis that HS phytoplankton communities follow a consistent successional pattern from diatoms to dinoflagellates is confirmed for summer but refuted for winter and remains a possibility for spring and fall. H2b, the hypothesis that diatom succession during all blooms in HS is characterized by large centric cells preceding small cells or pennate cells, is neither confirmed nor refuted and remains untested.

Evidence supporting the model of succession of diatoms to dinoflagellates proposed by Margalef (1978) was observed in summer but not in fall, winter, and spring. HS was a somewhat faithful model of how dinoflagellate growth is promoted in stratified and nutrient-poor summer conditions while diatom growth is promoted in well-mixed and nutrient-rich conditions the rest of the year, but there were exceptions. Small, brief, but significant diatom blooms occurred during summer stratification. Dinoflagellate blooms are out of phase with these diatom blooms, suggesting that diatom-to-dinoflagellate succession could be driven by episodic mixing events in an otherwise stratified and nutrient-limited water column. In contrast, dinoflagellate biovolume varied in phase outside the summer months; this suggests that turbulence and nutrients are not varying enough for Margalef's mandala to apply.

The investigation of ecological succession among diatom taxa is nuanced and unfinished. Taxa estimated to have had the largest cells on average (*Thalassiosira* and *Guinardia delicatula*)

reached peak biovolume first in 77% of the blooms observed (Table 1). This provides preliminary evidence that centric cells that tend to be larger are succeeded by smaller cells and pennate cells, as Kemp & Villareal (2018) predicts. Time of peak biovolume was estimated and could have been measured more accurately by normalizing the biovolume of each taxa to its peak biovolume achieved in each bloom.

The diatom taxa succession question is yet more complex because of the finding that populations of the same taxa can grow at different rates in different locations simultaneously. What appear to be successional sequences may be taxa developing in separate estuarine spaces simultaneously, revealing spatial dependence of phytoplankton composition. Now that it can be known how taxa develop in spatially independent populations within HS, presumably because of responses to different physical and biogeochemical structures, investigation of succession can treat these spaces separately.

In terrestrial plant ecosystems, each taxon faces an evolutionary trade-off between competing for resources, enduring resource limitation, and recovering from naturally occurring biomass destruction (Grime, 1977; Hutchings, 2021). Taxa may therefore evolve to be strong competitors, to be able to tolerate stress, or to be able to adapt to frequent disturbance (none of which is mutually exclusive). If an environment is nutrient limiting and reduces growth rates, none of the taxa may grow fast enough to outcompete the others (Tilman 1985). This may explain the abundant diversity of phytoplankton taxa despite competitive exclusion and similar requirements for limiting nutrients across species, known as the paradox of the plankton.

Diatom succession in HS may be analogous to terrestrial plant succession, random, or too complex to observe. Taxa dominance or bloom "take-off" may depend more on initial community composition than species traits and environmental drivers. Competitive ability might

be most selected for in *Thalassiosira* and *Guinardia delicatula* because they thrive during the nitrate- and silicate-rich conditions of winter, but they also bloom in summer, curiously. Stress tolerance might be selected for in cells during the low-nutrient summer, and ability to adapt to frequent disturbance might be selected for in cells year-round because predation pressure on HS phytoplankton remains underexplored. Zooplankton and mixotroph taxa graze on diatoms and reduce their populations by up to 20% per hour (Du Yoo et al. 2009; Figure S3). A genetic underpinning to succession was explored (Figure S4) but was out of the scope of this project.

### 6.3 Origin of diatom blooms

H3a, the hypothesis that HS, being a well-mixed coastal environment, has diatom populations that are uniformly distributed across space and will therefore exhibit no variability in concentration at the tidal cycle frequency, is refuted but acknowledged to occur sometimes. H3b (HS is seeded by robust seasonal diatom blooms detected in the GOM and thus shows greater high-tide diatom concentrations at the sampling location in spring and fall) and H3c (that the shallow coves of HS, being well-lit and well-mixed, act as incubators for diatom blooms and therefore show greater low-tide populations at the sampling location, regardless of seasonal physical changes to water column stability) are also refuted because of between-year, within-year, and between-taxa differences in onshore and offshore transport

Whether the bloom conditions are favorable offshore or onshore and promote transport from that location to HS is not consistent interannually. The *Guinardia delicatula* bloom of December 2021 through April 2022 appears to have initiated offshore and then concentrate onshore by the end of the bloom. The *Guinardia delicatula* bloom in March of 2021 had a consistently more concentrated low tide population, suggesting that instead of being imported from offshore like the early 2022 bloom, it was being incubated onshore. Moreover, the inferred

origin of blooms is not consistent across diatom taxa. During June 10th through 17th 2021, conditions that favor *Chaetoceros* growth offshore and that favor *Thalassiosira* growth onshore were observed. In other words, HS was seeded by offshore and onshore incubators simultaneously.

The decoupling of tidal endmember populations in spring blooms could be a product of the multiple pulses of inflowing freshwater at the surface concentrating the population in inner HS. Current regime switches to surface inflow cooccurred with spikes in upstream *Guinardia delicatula*. The same was observed in the instance in which the *Pseudonitzschia* bloom was impacted by inflowing freshwater. Usually as the current regime switched back to the baseline (inflow at depth and outflow at the surface) the onshore and offshore population concentrations equilibrated. Importantly, the observed *Pseudonitzschia* bloom in February 2022 and its presence onshore of the sampling location in HS indicates that potentially toxic species (notably *P. australis*) could reach significant biovolume in coastal areas during seasons other than summer and fall, when blooms have often been observed in the past decade (Clark et al. 2019). Propagation of concentrated *Pseudonitzschia* population may occur from within HS to other coastal regions depending on the favorability of the current regime.

#### 6.4 Changing composition of toxic blooms

H4a, the hypothesis that *Alexandrium* is the most concentrated toxic phytoplankton in HS, is refuted. H4b, the hypothesis that low-nutrient summer conditions facilitate toxic blooms in HS, with some blooms occurring earlier, is refuted because blooms of the dinoflagellates *Dinophysis acuminata* and *Heterocapsa triquetra*, and of the toxic diatom *Pseudonitzschia*, were observed in fall, winter, and early spring.

There is a large diversity in the toxic dinoflagellate suite that appears in HS, which includes *Heterocapsa triquetra*, *Dinophysis acuminata*, and *Karenia. Alexandrium catenella*, *Gonyaulax*, and *Dinophysis norvegica* biovolume contributions have been negligible in HS for the past 3 years, and *Heterocapsa triquetra* biovolume has decreased dramatically. Taxa that have increasingly shown up are *Dinophysis acuminata*, *Karenia* and the diatom *Pseudonitzschia*,

The genus *Pseudonitzschia*, which may include toxic species, appears to be growing in proportion to toxic dinoflagellates in this three-year interval. Moreover, *Pseudonitzschia* and *Dinophysis acuminata* were observed in significant concentration in January, February, March, and April, which are outside of the normal summer range of sampling for HABs.

The toxic dinoflagellate *Dinophysis acuminata* grows best in lower salinity water (22-26 ppm; Florendino et al. 2020), making HS, which has salinity in this range immediately following freshet intervals of the Kennebec River, particularly susceptible to blooms of this taxon during fall rains and especially during the early spring snowmelt. In spring 2022, there is evidence for a bloom of this taxa being imported to HS from onshore with the influx of lower salinity water. Shallow inland coves seem to be retentive incubators for growth of some phytoplankton taxa, such as *Dinophysis acuminata* in early spring and *Pseudonitzschia* in early spring and fall, which makes export of HABs from HS entirely possible.

The pattern of potential HABs and their movement recorded in HS is novel. Predictive models already state that the incidence of a HAB is more likely in a downwelling coastal current regime which transports cells onshore (<https://coastalscience.noaa.gov/science-areas/habs/hab-forecasts/gulf-of-maine-alexandrium-catenella-predictive-models/>) as occurs in the summer. McGillicuddy et al. (2003) predicted that "In the western Gulf of Maine, the offshore extent of the river plume during upwelling conditions is sufficient to entrain upward-swimming

*Alexandrium* cells germinated from offshore cyst beds. Subsequent downwelling conditions then transport those populations towards the coast." This may be true for the transition to summer downwelling conditions. However, IFCB evidence suggests that spring conditions may also be capable of transporting HABs from onshore to offshore in outgoing residual surface currents.

Blooms of *Dinophysis acuminata*, *Karenia*, and *Pseudonitzschia* are on the rise in fall and winter months in HS. This alone is cause for year-round predictive modeling reports of more taxa capable of producing toxins, not to mention that the spring bloom is coming earlier and earlier (Heike et al. 2022). The SCSC IFCB could be added as a tool for validating predictive models and monitoring HABs in real time.

### 6.5 Future directions

Lower mixing due to more thermal stratification could push the phytoplankton community from a diatom-dominated subarctic regime that it is today to a community dominated by smaller and less silicified taxa (Hieke et al. 2022). However, shifting nutrient ratios from the water entering the GOM seem to be conducive to diatom growth (Townsend et al. 2010), and increased temperature gradients between terrestrial and marine locations on the coast could increase winds and consequently increase mixing to the benefit of diatoms (Falkowski & Oliver 2007). More investigation is needed to establish the level of connection between offshore chlorophyll concentrations (observed using satellite and buoy data) and near-shore dynamics in diatom populations. However, it is certain that the inlets are their own ecosystem, separate from the shelf sea populations and greater in biomass. It is not well understood how the residual currents might strongly influence the ecosystem (Simpson et al. 2007) by dispersing or transporting phytoplankton in/out of the sound or causing mixing.

With each passing hour of IFCB data collection more research is possible. Partitioning phytoplankton communities into groups such as diatoms using satellite data and models is continuously improving, but it can be inaccurate in differentiating diatom abundance from the signals of other optical properties in coastal environments. Kramer et al. (2018) applied a modified existing model (Sathyendranath et al. 2004) to determine diatom dominance in Harpswell Sound through absorption and backscattering data, but the underlying assumptions were not robust for sites along the eastern seaboard, including HS. Satellite-based estimates of diatom carbon require in-situ validation from an instrument such as an IFCB. In the highly variable western North Atlantic, using satellite derived chlorophyll and IFCB data in a coupled neural network has been able to resolve diatom carbon across space at a finer spatial scale, but variation on the timescale of hours and the need to use composite multi-day satellite data impedes accuracy (Chase et al. 2022). The blooming dynamics and movement of diatoms within HS are complex, and support for the patterns observed here—or different findings—may emerge as more IFCB data is recorded over time and further analysis of that data is carried out.

## 7 Summary

This project evaluated the seasonality, succession, and location of origin of diatom blooms in Harpswell Sound.

1. There are spring and fall bloom features with multiple peaks. Summer diatom blooms were observed during net inflow in the upper 15 m and net outflow below 15 m, which is retentive flow. Winter diatom blooms were observed during net inflow below 5 m and net outflow above 5 m, which facilitates population broadcasting out of the inlet. Interannual variability in taxa comprising blooms and bloom timing was high. Import of the Kennebec River plume in spring decreased biovolume.
2. Diatom-to-dinoflagellate succession was observed in summer. What appear to be succession sequences or simultaneous blooms of different diatom taxa can be taxa developing in separate estuarine spaces (i.e., onshore or offshore). Currents and tides appear to control the import, export, retention, or nourishment of populations.
3. The toxic diatom *Pseudonitzschia* was observed increasing in concentration over the three-year study interval, and a notable bloom that originated at the head of the sound in February 2022 was observed. Blooms of *Dinophysis acuminata* and *Karenia* are also on the rise in fall and winter months in HS, suggesting that the SCSC IFCB could be added as a tool for validating predictive models and monitoring HABs in real time.

## Supplementary material

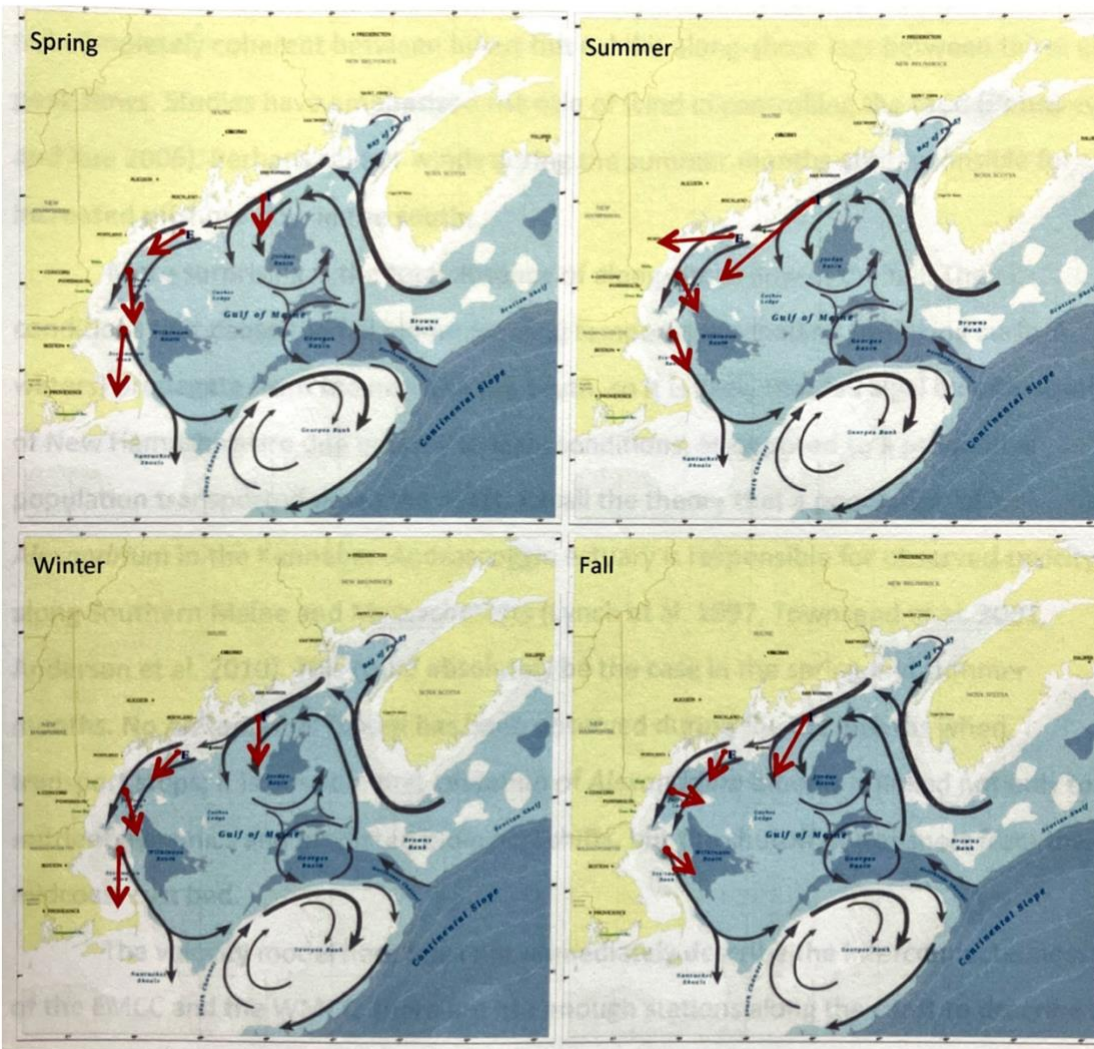


Figure S1. Seasonal average velocity vectors overlaid on the summer circulation model by Pettigrew et al. (2005) for each season (clockwise). Figure is Figure 16 from Peabody (2014).

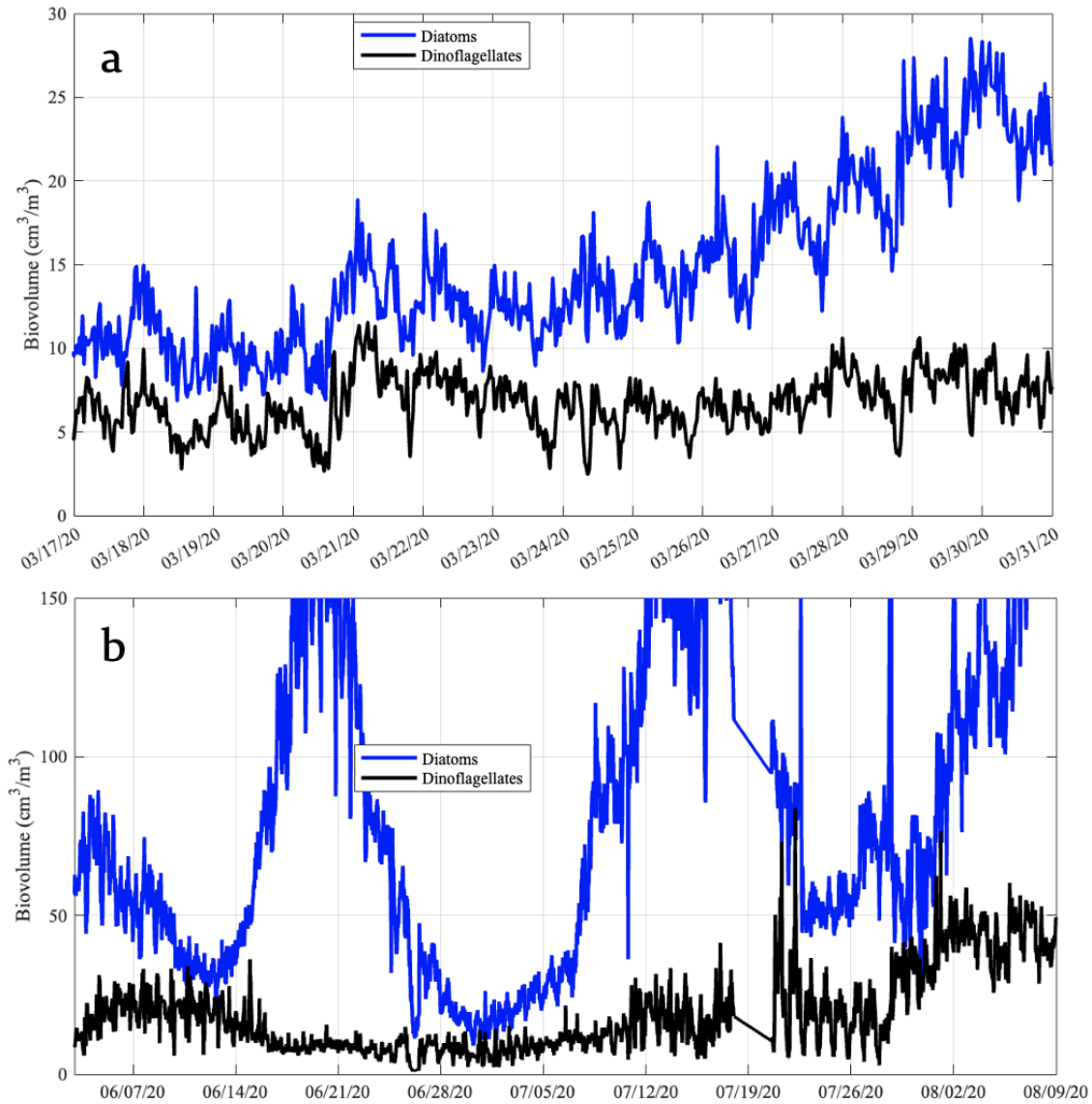
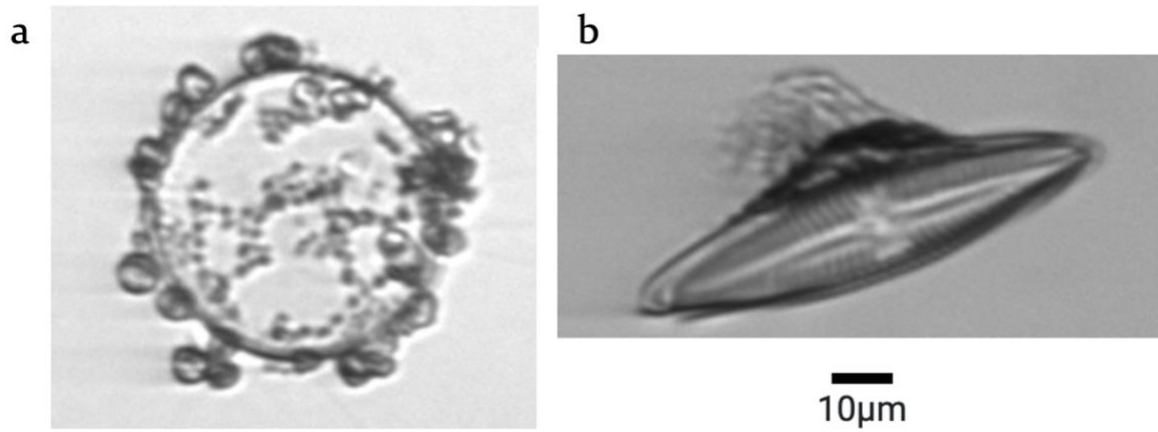


Figure S2. Notable examples of when dinoflagellate and diatom biovolume in Harpswell Sound are of similar magnitude, which occur in March (a), June, July, and August (b) of 2020.



*Figure S3. Example images of diatom interactions with detritivores and predators in HS. A centric diatom is decomposed by flagellates that have attached to the frustule (a; February 2021) and a pennate diatom is grazed upon by a ciliate (b; April 2021).*

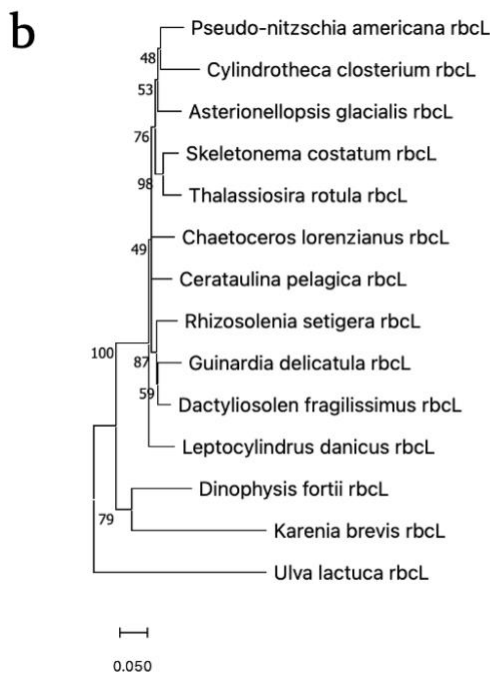
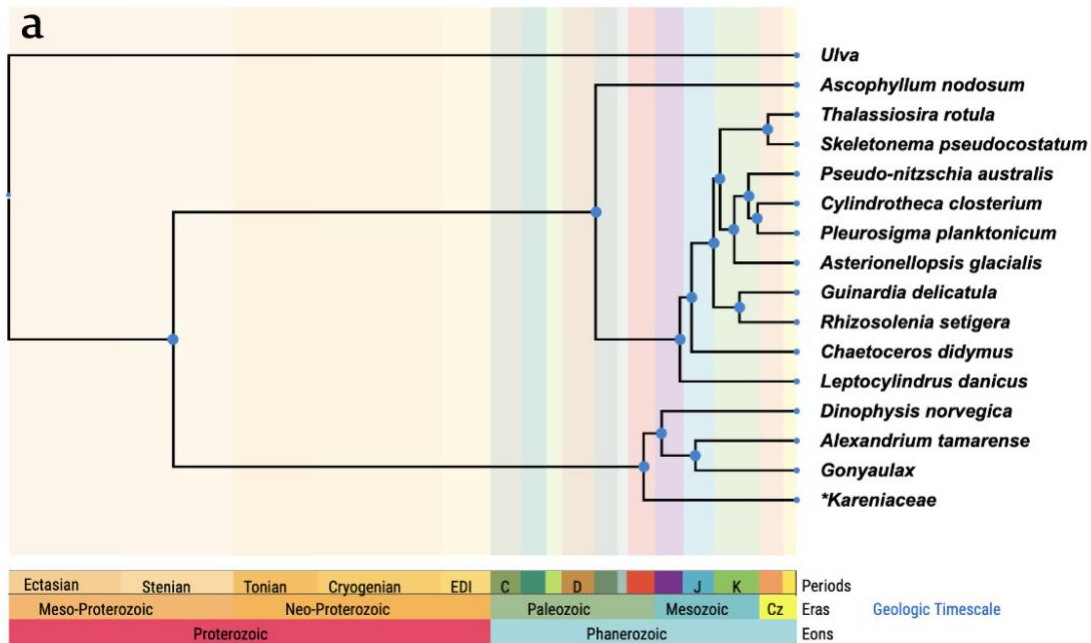


Figure S4. Phylogenetic trees of phytoplankton taxa in Harpswell Sound. Tree showing the divergence time of taxa from their most common ancestors (a; <http://www.timetree.org>; Ojha et al. 2022). \* denotes a replacement of Kareniaceae (the order of *Karenia brevis*) with Gymnodiniales, a closely related order. Neighbor-joining tree of the gene responsible for carbon-fixing enzyme Rubisco (rubulose-1,5-bisphosphate carboxylase/oxygenase large unit) of taxa available in the NCBI database that have the same geographic range as the taxa observed in Harpswell Sound and are the closest-related taxa according to the World Register of Marine Species (b). Number at each node is a measure of support (0-100) that the cluster excludes other taxa. The scale of genetic distance does not align with the geologic time scale of (a). Outgroups for (a) and (b) are the green alga *Ulva* (sea lettuce) and the brown alga *Ascophyllum nodosum* (rockweed).

## References

- Amin, S. A., Parker, M. S., & Armbrust, E. V. (2012). Interactions between diatoms and bacteria. *Microbiol Mol Biol Rev*, 76(3), 667-684. doi:10.1128/mmbr.00007-12
- Ansdell, V. (2019). 49 - Seafood Poisoning. In J. S. Keystone, P. E. Kozarsky, B. A. Connor, H. D. Nothdurft, M. Mendelson, & K. Leder (Eds.), *Travel Medicine (Fourth Edition)* (pp. 449-456). London: Elsevier.
- Armbrust, E. V. (2009). The life of diatoms in the world's oceans. *Nature*, 459(7244), 185-192. doi:10.1038/nature08057
- Ballance, S. B. (2020). Living Upstream: Kennebec River Influence on Nutrient Regimes and Phytoplankton Communities in Harpswell Sound. Bowdoin College Honors Projects, 209. Retrieved from <https://digitalcommons.bowdoin.edu/honorsprojects/209/>
- Bean, L. L., McGowan, J. D., & Hurst, J. W. (2005). Annual variations of paralytic shellfish poisoning in Maine, USA 1997–2001. *Deep Sea Research Part II: Topical Studies in Oceanography*, 52(19), 2834-2842. doi:<https://doi.org/10.1016/j.dsr2.2005.06.023>
- Benoiston, A.-S., Ibarbalz, F. M., Bittner, L., Guidi, L., Jahn, O., Dutkiewicz, S., & Bowler, C. (2017). The evolution of diatoms and their biogeochemical functions. *Philosophical Transactions of the Royal Society B: Biological Sciences*, 372(1728), 20160397. doi:10.1098/rstb.2016.0397
- Bolaños, L. M., Karp-Boss, L., Choi, C. J., Worden, A. Z., Graff, J. R., Haëntjens, N., . . . Giovannoni, S. J. (2020). Small phytoplankton dominate western North Atlantic biomass. *The ISME Journal*, 14(7), 1663-1674. doi:10.1038/s41396-020-0636-0
- Boyce, D. G., Lewis, M. R., & Worm, B. (2010). Global phytoplankton decline over the past century. *Nature*, 466(7306), 591-596. doi:10.1038/nature09268
- Carberry, L., Roesler, C., & Drapeau, S. (2019). Correcting in situ chlorophyll fluorescence time series observations for non-photochemical quenching and tidal variability reveals non-conservative phytoplankton variability in coastal waters. *Limnology and oceanography, methods*, 17. doi:10.1002/lom3.10325
- Chase, A. P., Boss, E. S., Haëntjens, N., Culhane, E., Roesler, C., & Karp-Boss, L. (2022). Plankton Imagery Data Inform Satellite-Based Estimates of Diatom Carbon. *Geophysical Research Letters*, 49(13), e2022GL098076. doi:<https://doi.org/10.1029/2022GL098076>
- Clark, S., Hubbard, K. A., Anderson, D. M., McGillicuddy, D. J., Ralston, D. K., & Townsend, D. W. (2019). Pseudo-nitzschia bloom dynamics in the Gulf of Maine: 2012–2016. *Harmful Algae*, 88, 101656. doi:<https://doi.org/10.1016/j.hal.2019.101656>
- Clark, S., Hubbard, K. A., McGillicuddy, D. J., Ralston, D. K., & Shankar, S. (2021). Investigating Pseudo-nitzschia australis introduction to the Gulf of Maine with observations and models. *Continental Shelf Research*, 228, 104493. doi:<https://doi.org/10.1016/j.csr.2021.104493>
- Cross, J., Nimmo-Smith, W. A. M., Hosegood, P. J., & Torres, R. (2015). The role of advection in the distribution of plankton populations at a moored 1-D coastal observatory. *Progress in Oceanography*, 137, 342-359. doi:<https://doi.org/10.1016/j.pocean.2015.04.016>
- D'Errico, J. (2023). `inpaint_nans`: MATLAB Central File Exchange. Retrieved from [https://www.mathworks.com/matlabcentral/fileexchange/4551-inpaint\\_nans](https://www.mathworks.com/matlabcentral/fileexchange/4551-inpaint_nans)
- Dawson, S. (2011). *Creatures from the Black Lagoon: Lessons in Diversity and Evolution of Eukaryotes*. Retrieved from <https://evrimteorisonline.com/2011/01/14/diversity-and-evolution-of-eukaryotes-by-scott-dawson/>

- Delwiche, C. F. (2007). CHAPTER 10 - The Origin and Evolution of Dinoflagellates. In P. G. Falkowski & A. H. Knoll (Eds.), *Evolution of Primary Producers in the Sea* (pp. 191-205). Burlington: Academic Press.
- DMR. (2022). Biotoxins in Maine. Retrieved from <https://www.maine.gov/dmr/fisheries/shellfish/bureau-of-public-health-programs/biotoxins-in-maine>
- Dolan, J. (1992). Mixotrophy in ciliates: A review of *Chlorella* symbiosis and chloroplast retention. *Marine Microbial Food Webs*, 6, 133-153.
- Du Yoo, Y., Jeong, H. J., Kim, M. S., Kang, N. S., Song, J. Y., Shin, W., . . . Lee, K. (2009). Feeding by phototrophic red-tide dinoflagellates on the ubiquitous marine diatom *Skeletonema costatum*. *J Eukaryot Microbiol*, 56(5), 413-420. doi:10.1111/j.1550-7408.2009.00421.x
- Evans, G. T., & Parslow, J. S. (1985). A Model of Annual Plankton Cycles. *Biological Oceanography*, 3(3), 327-347. doi:10.1080/01965581.1985.10749478
- Falkowski, P. G., & Oliver, M. J. (2007). Mix and match: how climate selects phytoplankton. *Nature Reviews: Microbiology*, 5, 813.
- Fiorendino, J. M., Smith, J. L., & Campbell, L. (2020). Growth response of *Dinophysis*, *Mesodinium*, and *Teleaulax* cultures to temperature, irradiance, and salinity. *Harmful Algae*, 98, 101896. doi:https://doi.org/10.1016/j.hal.2020.101896
- Flynn, K. J., Stoecker, D. K., Mitra, A., Raven, J. A., Glibert, P. M., Hansen, P. J., . . . Burkholder, J. M. (2012). Misuse of the phytoplankton–zooplankton dichotomy: the need to assign organisms as mixotrophs within plankton functional types. *Journal of Plankton Research*, 35(1), 3-11. doi:10.1093/plankt/fbs062
- Fong, D. A., Geyer, W. R., & Signell, R. P. (1997). The wind-forced response on a buoyant coastal current: Observations of the western Gulf of Maine plume. *Journal of Marine Systems*, 12(1), 69-81. doi:https://doi.org/10.1016/S0924-7963(96)00089-9
- Frangópulos, M., Guisande, C., DeBlas, E., & Maneiro, I. (2004). Toxin production and competitive abilities under phosphorus limitation of *Alexandrium* species. *Harmful Algae*, 3(2), 131-139.
- Gaul, W., & Antia, A. N. (2001). Taxon-specific growth and selective microzooplankton grazing of phytoplankton in the Northeast Atlantic. *Journal of Marine Systems*, 30(3), 241-261. doi:https://doi.org/10.1016/S0924-7963(01)00061-6
- Gemmell, B. J., Oh, G., Buskey, E. J., & Villareal, T. A. (2016). Dynamic sinking behaviour in marine phytoplankton: rapid changes in buoyancy may aid in nutrient uptake. *Proceedings of the Royal Society B: Biological Sciences*, 283(1840), 20161126. doi:10.1098/rspb.2016.1126
- Gilbert, P. M. (2016). Margalef revisited: A new phytoplankton mandala incorporating twelve dimensions, including nutritional physiology. *Harmful Algae*, 55, 25-30. doi:10.1016/j.hal.2016.01.008
- Gleason, H. A. (1926). The Individualistic Concept of the Plant Association. *Bulletin of the Torrey Botanical Club*, 53(1), 7-26. doi:10.2307/2479933
- Grime, J. P. (1977). Evidence for the Existence of Three Primary Strategies in Plants and Its Relevance to Ecological and Evolutionary Theory. *The American Naturalist*, 111(982), 1169-1194. Retrieved from <http://www.jstor.org/stable/2460262>

- Hankinson, S., Teegarden, G., Roesler, C., & Laine, E. (2010). Phytoplankton Dynamics in Harpswell Sound, Gulf of Maine. *Marine Lab Student Papers and Projects*, 7. Retrieved from <https://digitalcommons.bowdoin.edu/marinelab-student-papers/7/>
- Hennon, G. M. M., Ashworth, J., Groussman, R. D., Berthiaume, C., Morales, R. L., Baliga, N. S., . . . Armbrust, E. V. (2015). Diatom acclimation to elevated CO<sub>2</sub> via cAMP signalling and coordinated gene expression. *Nature Climate Change*, 5(8), 761-765. doi:10.1038/nclimate2683
- Hongo, Y., Kimura, K., Takaki, Y., Yoshida, Y., Baba, S., Kobayashi, G., . . . Tomaru, Y. (2021). The genome of the diatom *Chaetoceros tenuissimus* carries an ancient integrated fragment of an extant virus. *Scientific Reports*, 11(1), 22877. doi:10.1038/s41598-021-00565-3
- Hunter-Cevera, K., Neubert, M., Olson, R., Shalapyonok, A., Solow, A., & Sosik, H. (2019). Seasons of Syn. *Limnology and Oceanography*, 65. doi:10.1002/lno.11374
- Hutchings, J. (2021). *A Primer of Life Histories*: Oxford University Press.
- Irion, S., Christaki, U., Berthelot, H., L'Helguen, S., & Jardillier, L. (2021). Small phytoplankton contribute greatly to CO<sub>2</sub>-fixation after the diatom bloom in the Southern Ocean. *The ISME Journal*, 15(9), 2509-2522. doi:10.1038/s41396-021-00915-z
- Jang, J., Waite, W. F., Stern, L. A., & Lee, J. Y. (2022). Diatom influence on the production characteristics of hydrate-bearing sediments: Examples from Ulleung Basin, offshore South Korea. *Marine and Petroleum Geology*, 144, 105834. doi:<https://doi.org/10.1016/j.marpetgeo.2022.105834>
- Kemp, A. E. S., Pike, J., Pearce, R. B., & Lange, C. B. (2000). The “Fall dump” — a new perspective on the role of a “shade flora” in the annual cycle of diatom production and export flux. *Deep Sea Research Part II: Topical Studies in Oceanography*, 47(9), 2129-2154. doi:[https://doi.org/10.1016/S0967-0645\(00\)00019-9](https://doi.org/10.1016/S0967-0645(00)00019-9)
- Kemp, A. E. S., & Villareal, T. A. (2018). The case of the diatoms and the muddled mandalas: Time to recognize diatom adaptations to stratified waters. *Progress in Oceanography*, 167, 138-149. doi:<https://doi.org/10.1016/j.pocean.2018.08.002>
- Kimmerer, W. J., Gross, E. S., & MacWilliams, M. L. (2014). Tidal migration and retention of estuarine zooplankton investigated using a particle-tracking model. *Limnology and Oceanography*, 59(3), 901-916. doi:10.4319/lo.2014.59.3.0901
- Kramer, S. J., Roesler, C. S., & Sosik, H. M. (2018). Bio-optical discrimination of diatoms from other phytoplankton in the surface ocean: Evaluation and refinement of a model for the Northwest Atlantic. *Remote Sensing of Environment*, 217, 126-143. doi:<https://doi.org/10.1016/j.rse.2018.08.010>
- Li, D., Wang, Z., Xue, H., Thomas, A. C., & Etter, R. J. (2022). Wind-Modulated Western Maine Coastal Current and Its Connectivity with the Eastern Maine Coastal Current. *Journal of geophysical research: oceans*, 127(6). doi:10.1029/2022JC018469
- Lotze, H. K., Mellon, S., Coyne, J., Betts, M., Burchell, M., Fennel, K., . . . Kienast, M. (2022). Long-term ocean and resource dynamics in a hotspot of climate change. *FACETS*, 7, 1142-1184. doi:10.1139/facets-2021-0197
- Luostarinen, T., Ribeiro, S., Weckström, K., Sejr, M., Meire, L., Tallberg, P., & Heikkilä, M. (2020). An annual cycle of diatom succession in two contrasting Greenlandic fjords: from simple sea-ice indicators to varied seasonal strategists. *Marine Micropaleontology*, 158, 101873. doi:<https://doi.org/10.1016/j.marmicro.2020.101873>

- Madin, K. (2005). Building an Automated Underwater Microscope: A conversation with biologist Heidi Sosik. *Oceanus*. Retrieved from <https://www.whoi.edu/oceanus/feature/building-an-automated-underwater-microscope>
- Malviya, S., Scalco, E., Audic, S., Vincent, F., Veluchamy, A., Poulain, J., . . . Bowler, C. (2016). Insights into global diatom distribution and diversity in the world's ocean. *Proceedings of the National Academy of Sciences*, 113(11), E1516-E1525. doi:10.1073/pnas.1509523113
- Marchese, C., Hunt, B. P. V., Giannini, F., Ehrler, M., & Costa, M. (2022). Bioregionalization of the coastal and open oceans of British Columbia and Southeast Alaska based on Sentinel-3A satellite-derived phytoplankton seasonality. *Frontiers in Marine Science*, 9. doi:10.3389/fmars.2022.968470
- Margalef, R. (1978). Life-forms of phytoplankton as survival alternatives in an unstable environment. *Oceanologica Acta*, 1, 493-509.
- Martin, P., Lampitt, R. S., Jane Perry, M., Sanders, R., Lee, C., & D'Asaro, E. (2011). Export and mesopelagic particle flux during a North Atlantic spring diatom bloom. *Deep Sea Research Part I: Oceanographic Research Papers*, 58(4), 338-349. doi:<https://doi.org/10.1016/j.dsr.2011.01.006>
- Martinez, E., Antoine, D., D'Ortenzio, F., & de Boyer Montégut, C. (2011). Phytoplankton spring and fall blooms in the North Atlantic in the 1980s and 2000s. *Journal of geophysical research: oceans*, 116(C11). doi:<https://doi.org/10.1029/2010JC006836>
- Martínez-Cagigal, V. (2023). Custom Colormap. MATLAB Central File Exchange. Retrieved from <https://www.mathworks.com/matlabcentral/fileexchange/69470-custom-colormap>
- Mcgillicuddy, D. J., Jr, Signell, R. P., Stock, C. A., Keafer, B. A., Keller, M. D., Hetland, R. D., & Anderson, D. M. (2003). A mechanism for offshore initiation of harmful algal blooms in the coastal Gulf of Maine. *Journal of Plankton Research*, 25(9), 1131-1138. doi:10.1093/plankt/25.9.1131
- McLane. (2020). Imaging FlowCytobot User Manual. Retrieved from [https://mclanelabs.com/wp-content/uploads/2020/05/McLane-IFCB-Manual.Rev\\_.20.E.05.pdf](https://mclanelabs.com/wp-content/uploads/2020/05/McLane-IFCB-Manual.Rev_.20.E.05.pdf)
- Mouget, J.-L., Gastineau, R., Davidovich, O., Gaudin, P., & Davidovich, N. A. (2009). Light is a key factor in triggering sexual reproduction in the pennate diatom *Haslea ostrearia*. *FEMS Microbiology Ecology*, 69(2), 194-201. doi:10.1111/j.1574-6941.2009.00700.x
- Nardelli, S., & Roesler, C. (2014). Using data from the LISST-100 to recreate phytoplankton size distribution and processes in Harpswell Sound, Maine.
- Ojha, K. K., Mishra, S., & Singh, V. K. (2022). Chapter 5 - Computational molecular phylogeny: concepts and applications. In D. B. Singh & R. K. Pathak (Eds.), *Bioinformatics* (pp. 67-89): Academic Press.
- Olson, R. J., Sosik, H. (2007). A submersible imaging-in-flow instrument to analyze nano- and microplankton: Imaging FlowCytobot. *Limnology and Oceanography: Methods*(5), 193-203.
- Peabody, R. (2014). Coastal Currents in the Gulf of Maine: a Mechanism for Algal Transport. Bowdoin College Honors Projects.
- Pettigrew, N. R., Churchill, J. H., Janzen, C. D., Mangum, L. J., Signell, R. P., Thomas, A. C., . . . Xue, H. (2005). The kinematic and hydrographic structure of the Gulf of Maine Coastal Current. *Deep Sea Research Part II: Topical Studies in Oceanography*, 52(19), 2369-2391. doi:<https://doi.org/10.1016/j.dsr2.2005.06.033>

- Ruggiero, M. V., Kooistra, W. H. C. F., Piredda, R., Sarno, D., Zampicinini, G., Zingone, A., & Montresor, M. (2022). Temporal changes of genetic structure and diversity in a marine diatom genus discovered via metabarcoding. *Environmental DNA*, 4(4), 763-775. doi:<https://doi.org/10.1002/edn3.288>
- Sathyendranath, S., Watts, L., Devred, E., Platt, T., Caverhill, C., & Maass, H. (2004). Discrimination of diatoms from other phytoplankton using ocean-colour data. *Marine Ecology-progress Series - MAR ECOL-PROGR SER*, 272, 59-68. doi:10.3354/meps272059
- Selander, E., Thor, P., Toth, G., & Pavia, H. (2006). Copepods induce paralytic shellfish toxin production in marine dinoflagellates. *Proceedings of the Royal Society B: Biological Sciences*, 273(1594), 1673-1680.
- Shukla, S., & Mohan, R. (2012). The Contribution of Diatoms to Worldwide Crude Oil Deposits. In (Vol. 25, pp. 355-382).
- Simpson, J. H., Berx, B., Gascoigne, J., & Saurel, C. (2007). The interaction of tidal advection, diffusion and mussel filtration in a tidal channel. *Journal of Marine Systems*, 68(3), 556-568. doi:<https://doi.org/10.1016/j.jmarsys.2007.02.021>
- Simpson, J. H., & Sharples, J. (2012). *Introduction to the Physical and Biological Oceanography of Shelf Seas*. Cambridge University Press.
- Song, H., Ji, R., Stock, C., & Wang, Z. (2010). Phenology of phytoplankton blooms in the Nova Scotian Shelf–Gulf of Maine region: remote sensing and modeling analysis. *Journal of Plankton Research*, 32(11), 1485-1499. doi:10.1093/plankt/fbq086
- Sosik, H. (2014). Annotated Plankton Images - Data Set for Development and Evaluation of Classification Methods. Retrieved from: <https://whoigit.github.io/whoiplankton/index.html>
- Sosik, H. M., Olson, R. (2007). Automated taxonomic classification of phytoplankton sampled with imaging in-flow cytometry. *Limnology and Oceanography: Methods*(5), 204-216.
- Sosik, H. M., Green, R. E., Pegua, W. S., & Roseler, C. S. (2001). Temporal and vertical variability in optical properties of New England shelf waters during late summer and spring. *Journal of geophysical research: oceans*, 106(9455-9472).
- Suzuki, K., Yoshino, Y., Nosaka, Y., Nishioka, J., Hooker, S. B., & Hirawake, T. (2021). Diatoms contributing to new production in surface waters of the northern Bering and Chukchi Seas during summer with reference to water column stratification. *Progress in Oceanography*, 199, 102692. doi:<https://doi.org/10.1016/j.pocean.2021.102692>
- Sverdrup, H. U. (1953). On Conditions for the Vernal Blooming of Phytoplankton. *ICES Journal of Marine Science*, 18(3), 287-295. doi:10.1093/icesjms/18.3.287
- Tilman, D. (1985). The Resource-Ratio Hypothesis of Plant Succession. *The American Naturalist*, 125(6), 827-852. Retrieved from <http://www.jstor.org/stable/2461449>
- Townsend, D. W., Rebuck, N. D., Thomas, M. A., Karp-Boss, L., & Gettings, R. M. (2010). A changing nutrient regime in the Gulf of Maine. *Continental Shelf Research*, 30(7), 820-832. doi:<https://doi.org/10.1016/j.csr.2010.01.019>
- Tulan, E., Radl, M., Sachsenhofer, R., Tari, G., & Witkowski, J. (2020). Hydrocarbon source rock potential of Miocene diatomaceous sequences in Szurdokpüspöki (Hungary) and Parisdorf/Limberg (Austria). *Austrian Journal of Earth Sciences*, 113, 24-42. doi:10.17738/ajes.2020.0002
- Valbi, E., Ricci, F., Capellacci, S., Casabianca, S., Scardi, M., & Penna, A. (2019). A model predicting the PSP toxic dinoflagellate *Alexandrium minutum* occurrence in the coastal

- waters of the NW Adriatic Sea. *Scientific Reports*, 9(1), 4166. doi:10.1038/s41598-019-40664-w
- Westacott, S., Planavsky, N. J., Zhao, M.-Y., & Hull, P. M. (2021). Revisiting the sedimentary record of the rise of diatoms. *Proceedings of the National Academy of Sciences*, 118(27), e2103517118. doi:10.1073/pnas.2103517118
- Whitney, N. M., Wanamaker, A. D., Ummenhofer, C. C., Johnson, B. J., Cresswell-Clay, N., & Kreutz, K. J. (2022). Rapid 20th century warming reverses 900-year cooling in the Gulf of Maine. *Communications Earth & Environment*, 3(1), 179. doi:10.1038/s43247-022-00504-8
- WHOI. (2019). Diarrhetic Shellfish Poisoning. Harmful Algae. Retrieved from <https://hab.whoi.edu/impacts/impacts-human-health/human-health-diarrhetic-shellfish-poisoning/>
- Wirtz, K., Smith, S. L., Mathis, M., & Taucher, J. (2022). Vertically migrating phytoplankton fuel high oceanic primary production. *Nature Climate Change*, 12(8), 750-756. doi:10.1038/s41558-022-01430-5
- Wolovick, M., Laine, E., Roesler, C., & Teegarden, G. (2008). The influence of the Kennebec River discharge on estuarine and reverse estuarine flow in eastern Casco Bay, Gulf of Maine. American Geophysical Union Fall Meeting Abstract, OS21B-1177.
- Yelton, R., Slaughter, A. M., & Kimmerer, W. J. (2022). Diel Behaviors of Zooplankton Interact with Tidal Patterns to Drive Spatial Subsidies in the Northern San Francisco Estuary. *Estuaries and Coasts*, 45(6), 1728-1748. doi:10.1007/s12237-021-01036-8
- Yoshida, T., Hairston, N. G., & Ellner, S. P. (2004). Evolutionary trade-off between defence against grazing and competitive ability in a simple unicellular alga, *Chlorella vulgaris*. *Proceedings of the Royal Society of London. Series B: Biological Sciences*, 271(1551), 1947-1953. doi:10.1098/rspb.2004.2818
- Zheng, Y., Gong, X., & Gao, H. (2022). Selective grazing of zooplankton on phytoplankton defines rapid algal succession and blooms in oceans. *Ecological Modelling*, 468, 109947. doi:https://doi.org/10.1016/j.ecolmodel.2022.109947